Geographic variability in freshwater methane hydrogen isotope ratios and its implications for global isotopic source signatures

Peter M.J. Douglas[1], Emerald Stratigopoulos[1*], Jenny Park[1], Dawson Phan[1]

[1]Earth and Planetary Sciences, McGill University, Montreal, H3A 0E8, Canada
* Now at Department of Earth Sciences, University of Toronto, Toronto, M5S 3B1, Canada

Correspondence to: Peter M. J. Douglas (peter.douglas@mcgill.ca)

Abstract. There is growing interest in developing spatially resolved methane (CH_4) isotopic source signatures to aid in geographic source attribution of CH_4 emissions. CH_4 hydrogen isotope measurements ($\delta^2H\text{-}CH_4$) have the potential to be a powerful tool for geographic differentiation of CH_4 emissions from freshwater environments, as well as other microbial sources. This is because microbial $\delta^2H\text{-}CH_4$ values are partially dependent on the δ^2H of environmental water ($\delta^2H\text{-}H_2O$), which exhibits large and well-characterized spatial variability globally. We have refined the existing global relationship between $\delta^2H\text{-}CH_4$ and $\delta^2H\text{-}H_2O$ by compiling a more extensive global dataset of $\delta^2H\text{-}CH_4$ from freshwater environments, including wetlands, inland waters, and rice paddies, comprising a total of 129 different sites, and compared these with measurements and estimates of $\delta^2H\text{-}H_2O$, as well as $\delta^{13}C\text{-}CH_4$ and $\delta^{13}C\text{-}CO_2$ measurements. We found that estimates of $\delta^2H\text{-}H_2O$ explain approximately 42% of the observed variation in $\delta^2H\text{-}CH_4$, with a flatter slope than observed in previous studies. The inferred global $\delta^2H\text{-}CH_4$ vs. $\delta^2H\text{-}H_2O$ regression relationship is not sensitive to using either modelled precipitation δ^2H or measured $\delta^2H\text{-}H_2O$ as the predictor variable. The slope of the global freshwater relationship between $\delta^2H\text{-}CH_4$ and $\delta^2H\text{-}H_2O$ is similar to observations from incubation experiments, but is different from pure culture experiments. This result is consistent with previous suggestions that variation in the δ^2H of acetate, controlled by environmental $\delta^2H\text{-}H_2O$, is important in determining variation in $\delta^2H\text{-}CH_4$. The relationship between $\delta^2H\text{-}CH_4$ and $\delta^2H\text{-}H_2O$ leads to significant differences in the distribution of freshwater $\delta^2H\text{-}CH_4$ between the northern high latitudes (60-90ºN), relative to other global regions. We estimate a flux-weighted global freshwater $\delta^2H\text{-}CH_4$ of -310±15‰, which is higher than most previous estimates. Comparison with $\delta^{13}C$ measurements of both CH_4 and CO_2 implies that residual $\delta^2H\text{-}CH_4$ variation is the result of complex interactions between CH_4 oxidation, variation in the dominant pathway of methanogenesis, and potentially other biogeochemical variables. We observe a significantly greater distribution of $\delta^2H\text{-}CH_4$ values, corrected for $\delta^2H\text{-}H_2O$, in inland waters relative to wetlands, and suggest this difference is caused by more prevalent CH_4 oxidation in inland waters. We used the expanded freshwater CH_4 isotopic dataset to calculate a bottom-up estimate of global source $\delta^2H\text{-}CH_4$ and $\delta^{13}C\text{-}CH_4$ that includes spatially resolved isotopic signatures for freshwater CH_4 sources. Our bottom-up global source $\delta^2H\text{-}CH_4$ estimate (-278±15‰) is higher than a previous estimate using a similar approach, as a result of the more enriched global freshwater $\delta^2H\text{-}CH_4$ signature derived from our dataset. However, it is

52 in agreement with top-down estimates of global source δ^2H-CH$_4$ based on atmospheric measurements and estimated

53 atmospheric sink fractionations. In contrast our bottom-up global source δ^{13}C-CH$_4$ estimate is lower than top-down

54 estimates, partly as a result of a lack of δ^{13}C-CH$_4$ data from C$_4$ plant dominated ecosystems. In general, we find there is a

55 particular need for more data to constrain isotopic signatures for low-latitude microbial CH$_4$ sources.

56 **1 Introduction**

57 Methane (CH$_4$) is an important greenhouse gas that accounts for approximately 25% of current anthropogenic global

58 warming, but we do not have a complete understanding of the current relative or absolute fluxes of different CH$_4$ sources

59 to the atmosphere (Schwietzke et al., 2016;Saunois et al., 2019), nor is there consensus on the causes of recent decadal-

60 scale changes in the rate of increase in atmospheric CH$_4$ (Kai et al., 2011;Pison et al., 2013;Rice et al., 2016;Schaefer et

61 al., 2016;Worden et al., 2017;Thompson et al., 2018;Turner et al., 2019). Freshwater ecosystems are an integral

62 component of the global CH$_4$ budget. They are one of the largest sources of atmospheric CH$_4$ and are unequivocally the

63 largest natural, or non-anthropogenic, source (Bastviken et al., 2011;Saunois et al., 2019). At the same time the

64 geographic distribution of freshwater CH$_4$ emissions, changes in the strength of this source through time, and the relative

65 importance of wetland versus inland water CH$_4$ emissions all remain highly uncertain (Pison et al., 2013;Schaefer et al.,

66 2016;Ganesan et al., 2018;Saunois et al., 2019;Turner et al., 2019). Gaining a better understanding of freshwater CH$_4$

67 emissions on a global scale is of great importance for understanding potential future climate feedbacks related to CH$_4$

68 emissions from these ecosystems (Bastviken et al., 2011;Koven et al., 2011;Yvon-Durocher et al., 2014;Zhang et al.,

69 2017). It is also necessary in order to better constrain the quantity and rate of change of other CH$_4$ emissions sources,

70 including anthropogenic sources from fossil fuels, agriculture, and waste (Kai et al., 2011;Pison et al., 2013;Schaefer et

71 al., 2016).

72 Isotopic tracers, particularly δ^{13}C, have proven to be very useful in constraining global CH$_4$ sources and sinks

73 (Kai et al., 2011;Nisbet et al., 2016;Rice et al., 2016;Schaefer et al., 2016;Schwietzke et al., 2016;Nisbet et al., 2019).

74 However, δ^{13}C source signatures cannot fully differentiate CH$_4$ sources, leaving residual ambiguity in source

75 apportionment (Schaefer et al., 2016;Schwietzke et al., 2016;Worden et al., 2017;Turner et al., 2019). Applying

76 additional isotopic tracers to atmospheric CH$_4$ monitoring has the potential to greatly improve our understanding of CH$_4$

77 sources and sinks (Turner et al., 2019; Saunois et al., 2020). Recently developed laser-based methods, including cavity

78 ringdown spectroscopy, quantum cascade laser absorption spectroscopy, and tunable infrared laser direct absorption

79 spectroscopy, in addition to continued application of isotope ratio mass spectrometry (Chen et al., 2016; Röckmann et al.,

80 2016; Yacovitch et al., 2020) could greatly enhance the practicality of atmospheric δ^2H-CH$_4$ measurements at greater

81 spatial and temporal resolution, similar to recent developments for δ^{13}C-CH$_4$ measurements (Zazzeri et al., 2015; Miles et

82 al., 2018). δ^2H-CH$_4$ measurements have proven useful in understanding past CH$_4$ sources in ice-core records (Whiticar

Peter Douglas 5/13/2021 12:20 PM

and Schaefer, 2007; Mischler et al., 2009; Bock et al., 2010; Bock et al., 2017), but have seen only limited use in modern atmospheric CH_4 budgets (Kai et al., 2011; Rice et al., 2016), in part because of loosely constrained source terms, as well as relatively sparse atmospheric measurements. Atmospheric inversion models have shown that increased spatial and temporal resolution of δ^2H-CH_4 measurements could provide substantial improvements in precision for global and regional methane budgets (Rigby et al., 2012).

δ^2H-CH_4 measurements could prove especially useful in understanding freshwater CH_4 emissions. Freshwater δ^2H-CH_4 is thought to be highly dependent on δ^2H-H_2O (Waldron et al., 1999a; Whiticar, 1999; Chanton et al., 2006). Since δ^2H-H_2O exhibits large geographic variation as a function of temperature and fractional precipitation (Rozanski et al., 1993; Bowen and Revenaugh, 2003), δ^2H-CH_4 measurements have the potential to differentiate freshwater CH_4 sources by latitude. This approach has been applied in some ice core studies (Whiticar and Schaefer, 2007; Bock et al., 2010), but geographic source signals remain poorly constrained, in part because of small datasets and because of incompletely understood relationships between δ^2H-H_2O and δ^2H-CH_4. In contrast, recent studies of modern atmospheric δ^2H-CH_4 have typically not accounted for geographic variation in freshwater CH_4 sources (Kai et al., 2011; Rice et al., 2016). Relatedly, other studies have found an important role for variation in δ^2H-H_2O in controlling δ^2H-CH_4 from biomass burning (Umezawa et al., 2011) and from plants irradiated by UV light (Vigano et al., 2010), as well as the δ^2H of H_2 produced by wood combustion (Röckmann et al., 2016).

In addition to variance caused by δ^2H-H_2O, a number of additional biogeochemical variables have been proposed to influence δ^2H-CH_4 in freshwater environments. These include differences in the predominant biochemical pathway of methanogenesis (Whiticar et al., 1986; Whiticar, 1999; Chanton et al., 2006), the extent of methane oxidation (Happell et al., 1994; Waldron et al., 1999a; Whiticar, 1999; Cadieux et al., 2016), isotopic fractionation resulting from diffusive gas transport (Waldron et al., 1999a; Chanton, 2005), and differences in the thermodynamic favorability or enzymatic reversibility of methanogenesis (Valentine et al., 2004b; Stolper et al., 2015; Douglas et al., 2016). These influences on δ^2H-CH_4 have the potential to complicate geographic signals, but also provide the potential to differentiate ecosystem sources, if specific ecosystems are characterized by differing rates and pathways of methanogenesis, rates of CH_4 oxidation, or gas transport processes. A recent study proposed that freshwater $\delta^{13}C$-CH_4 could be differentiated geographically based on ecosystem differences in the prevalence of different methanogenic pathways and in the predominance of C_4 plants, in addition to the geographic distribution of wetland ecosystems (Ganesan et al., 2018). δ^2H-CH_4 measurements have the potential to complement this approach by providing an additional isotopic parameter for differentiating ecosystem and geographic CH_4 source signatures.

In order to use δ^2H-CH_4 as an indicator of freshwater ecosystem contributions to global and regional CH_4 emissions budgets, a clearer understanding of freshwater δ^2H source signals, and how they vary by geographic location, ecosystem type, and other variables is needed. In order to address this need we have assembled and analyzed a dataset of 897 δ^2H-CH_4 measurements from 129 individual ecosystems, or sites, derived from 40 publications (Schoell, 1983;

117 Woltemate et al., 1984; Burke Jr and Sackett, 1986; Whiticar et al., 1986; Burke Jr et al., 1988; Burke Jr, 1992; Burke Jr
118 et al., 1992 ;Lansdown et al., 1992; Lansdown, 1992; Martens et al., 1992; Wassmann et al., 1992; Happell et al., 1993;
119 Levin et al., 1993; Happell et al., 1994; Wahlen, 1994; Bergamaschi, 1997; Chanton et al., 1997; Hornibrook et al., 1997;
120 Tyler et al., 1997; Zimov et al., 1997; Bellisario et al., 1999; Popp et al., 1999; Waldron et al., 1999b; Chasar et al., 2000;
121 Marik et al., 2002; Nakagawa et al., 2002b; Nakagawa et al., 2002a; Chanton et al., 2006; Walter et al., 2006; Walter et
122 al., 2008; Alstad and Whiticar, 2011; Brosius et al., 2012; Sakagami et al., 2012; Bouchard et al., 2015; Stolper et al.,
123 2015; Wang et al., 2015; Cadieux et al., 2016; Douglas et al., 2016; Thompson et al., 2016; Lecher et al., 2017). We have
124 advanced existing datasets of freshwater δ^2H-CH$_4$ (Whiticar et al., 1986; Waldron et al., 1999a; Sherwood et al., 2017) in
125 the following key attributes:_1) compiling a significantly larger dataset than was previously available; 2) compiling
126 paired δ^{13}C-CH$_4$ data for all sites, δ^{13}C-CO$_2$ data for 50% of sites, and δ^2H-H$_2$O data for 47% of sites; 3) compiling
127 geographic coordinates for all sites, providing the ability to perform spatial analyses and compare with gridded datasets
128 of precipitation isotopic composition; and 4) classifying all sites by ecosystem and sample type (dissolved vs. gas
129 samples), allowing for a clearer differentiation of how these variables influence δ^2H-CH$_4$.

130 Using this data set we applied statistical analyses to address key questions surrounding the global distribution of
131 freshwater δ^2H-CH$_4$, the variables that control this distribution, and its implications for atmospheric δ^2H-CH$_4$.
132 Specifically, we investigated the nature of the global dependence of δ^2H-CH$_4$ on δ^2H-H$_2$O, and whether this relationship
133 results in significant differences in freshwater δ^2H-CH$_4$ by latitude. We also assessed whether variability in δ^{13}C-CH$_4$,
134 δ^{13}C-CO$_2$, and α_C was correlated with δ^2H-CH$_4$, and whether there are significant differences in δ^2H-CH$_4$ between
135 different ecosystem and sample types. Finally, we used our dataset, combined with other isotopic datasets (Sherwood et
136 al., 2017) and flux estimates (Saunois et al., 2020), to estimate the global δ^2H-CH$_4$ and δ^{13}C-CH$_4$ of global emissions
137 sources, and compared this with previous estimates based on atmospheric measurements or isotopic datasets (Whiticar
138 and Schaefer, 2007;Rice et al., 2016;Sherwood et al., 2017),.

139 **2 Methods**

140 **2.1 Isotope Nomenclature**

141 Hydrogen and carbon isotope ratios are primarily discussed as delta values, using the generalized formula (Coplen,
142 2011):

143
$$\delta = \frac{\left(R_{sample} - R_{standard}\right)}{R_{standard}} \tag{1}$$

144 where R is the ratio of the heavy isotope to the light isotope, and the standard is Vienna Standard Mean Ocean Water
145 (VSMOW) for δ^2H and Vienna Pee Dee Belemnite (VPDB) for δ^{13}C. δ values are expressed in per mil (‰) notation.

Peter Douglas 5/11/2021 9:42 AM

Peter Douglas 5/17/2021 2:00 PM

Peter Douglas 5/11/2021 9:43 AM

149    We also refer to the isotopic fractionation factor between two phases, or α, which is defined as:

150 $$\alpha_{a-b} = \frac{R_a}{R_b} = \frac{\delta_a + 1}{\delta_b + 1}$$    (2)

151 Specifically, we discuss the carbon isotope fractionation factor between CO_2 and CH_4 (α_C) and the hydrogen isotope

152 fractionation factor between H_2O and CH_4 (α_H).

2.2 Dataset Compilation

2.2.1 Literature Survey

155 To identify datasets we used a set of search terms (methane OR CH_4 AND freshwater OR wetland OR peatland OR

156 swamp OR marsh OR lake OR pond OR 'inland water' AND 'hydrogen isotope' OR 'δD' OR 'δ^{2}H') in Google Scholar

157 to find published papers that discussed this measurement. We also identified original publications using previously

158 compiled datasets (Waldron et al., 1999a;Sherwood et al., 2017). Data for 90% of sites were from peer-reviewed

159 publications. Data from 13 sites were from a Ph.D. dissertation (Lansdown, 1992).

2.2.2 Dataset structure

161 Most samples were associated with geographic coordinates in data tables or text documentation, or with specific

162 geographic locations such as the name of a town or city. In a few cases we identified approximate geographic locations

163 based on text descriptions of sampling sites, with the aid of Google Earth software. Sampling sites were defined as

164 individual water bodies or wetlands as identified in the relevant study. In one study where a number of small ponds were

165 sampled from the same location, we grouped ponds of a given type as a single site (Bouchard et al., 2015). We divided

166 sampling sites into six ecosystem categories: 1) lakes and ponds (hereafter lakes), 2) rivers and floodplains (hereafter

167 rivers), 3) bogs, 4) fens, 5) swamps and marshes, and 6) rice paddies. Most data (7 of 8 sites) in the rivers category are

168 from floodplain lake or delta environments. Swamps and marshes were combined as one category because of a small

169 number of sites, and because there is no clear indication of biogeochemical differences between these ecosystems. To

170 make these categorizations we relied on site descriptions in the data source publications. We also analyzed data in two

171 larger environment types, inland waters (lakes and rivers) and wetlands (bogs, fens, swamps and marshes, and rice

172 paddies), which correspond to two flux categories (freshwaters and natural wetlands) documented by Saunois et al.

173 (2020). While rice paddies are an anthropogenic ecosystem, they are wetlands where microbial methanogenesis occurs

174 under generally similar conditions to natural wetlands, and therefore we included them as wetlands in our analysis. In

175 some cases the type of wetland was not specified. We did not differentiate between ombrotrophic and minerotrophic

176 peatlands since most publications did not specify this difference, although it has been inferred to be important for δ^{13}C-

Peter Douglas 5/11/2021 1:46 PM

CH$_4$ distributions (Hornibrook, 2009). For studies of bogs and fens that sampled by soil depth we have only included sample measurements from the upper 50 cm. This is based on the observation of large-scale isotopic variability with soil depth in these ecosystems (Hornibrook et al., 1997;Waldron et al., 1999b), and the observation that shallow peat is typically the dominant source of atmospheric emissions (Waldron et al., 1999b;Bowes and Hornibrook, 2006;Shoemaker et al., 2012), which is our primary focus in this study. Other wetland ecosystems were not sampled by soil depth.

We also categorized samples by the form in which CH$_4$ was sampled, differentiating between dissolved CH$_4$ and CH$_4$ emitted through diffusive fluxes, which we group as dissolved CH$_4$, and gas-phase samples, including bubbles sampled either by disturbing sediments or by collecting natural ebullition fluxes. In some cases the sampling method or type of sample was not specified, or samples were a mix of both categories, which we did not attempt to differentiate.

Where possible (78% of sites), δ^2H-CH$_4$ and δ^{13}C-CH$_4$ values, as well as δ^{13}C-CO$_2$ and δ^2H-H$_2$O, were gathered from data files or published tables. In a number of publications, representing 22% of sites, data were only available graphically. For these studies we used Webplot Digitizer (https://automeris.io/WebPlotDigitizer/) software to extract data for these parameters. Previous studies have shown that user errors from Webplot Digitizer are typically small, with 90% of user generated data within 1% of the actual value (Drevon et al., 2017). Based on this, we estimate a typical error for δ^2H-CH$_4$ data of less than 3‰. Studies where data were derived from graphs are identified in Supplementary Table S1 (Douglas et al., 2020).

2.2.3 Estimates of δ^2H-H$_2$O and its effects on δ^2H-CH$_4$

To estimate δ^2H-H$_2$O for sites where it was not measured we relied on estimates of the isotopic composition of precipitation (δ^2H$_p$), derived from the Online Isotopes in Precipitation Calculator v.3.1 (OIPC3.1; www.waterisotopes.org; Bowen and Wilkinson, 2002; Bowen and Revenaugh, 2003; Bowen et al., 2005). Inputs for δ^2H$_p$ estimates are latitude, longitude, and elevation. We estimated elevation for each site surface elevation at the site's geographic coordinates reported by Google Earth. We tabulated estimates of both annual and growing season precipitation-amount weighted δ^2H$_p$, where the growing season is defined as months with a mean temperature greater than 0 ºC. We then analysed whether annual or growing season δ^2H$_p$ is a better estimate of environmental δ^2H-H$_2$O for both wetlands and inland waters by comparing these values with measured δ^2H-H$_2$O for sites with measurements (See Sect. 3.2). Based on this analysis, we then identified a 'best-estimate' δ^2H-H$_2$O value for each site, using an approach similar to that of Waldron et al. (1999a). Namely, we apply measured δ^2H-H$_2$O where available, and estimates based on the regression analyses detailed in Section 3.2 for sites without measurements.

To account for the effects of δ^2H-H$_2$O on δ^2H-CH$_4$, we introduce the term δ^2H-CH$_{4,W0}$, which is the estimated δ^2H-CH$_4$ of a sample if it had formed in an environment where δ^2H-H$_2$O = 0‰. This is defined by the equation:

$$\delta^2\text{H-CH}_{4,W0} = \delta^2\text{H-CH}_4 - \left(b \times \delta^2\text{H}_2\text{O}\right) \tag{3}$$

where δ^2H-H$_2$O is the 'best-estimate' value for each site described above, b is the slope of the regression relationship of δ^2H-H$_2$O vs. δ^2H-CH$_4$ for the entire dataset, as reported in Sect. 3.3. We also performed the same calculation separately for the subset of sites with measured δ^2H-H$_2$O. We analyze δ^2H-CH$_{4,W0}$ instead of α_H because, as discussed in Sect. 3.3.1, the global relationship between δ^2H$_p$ vs. δ^2H-CH$_4$ does not correspond to a constant value of α_H, and therefore deviations from the global empirical relationship are more clearly expressed as a residual as opposed to a fractionation factor.

2.3 Statistical analyses

For all statistical analyses we use site-level mean isotopic values. This avoids biasing our analyses towards sites with a large number of measurements, since there are large differences in the number of samples analyzed per site (n ranges from 66 to 1). To calculate α_C we used average δ^{13}C-CH$_4$ and δ^{13}C-CO$_2$ at a given site. This approach entails some additional uncertainty in this variable, but was necessary because at many sites these measurements were not made on the same samples.

We perform a set of linear regression analyses δ^2H-CH$_4$ against other isotopic variables, in addition to latitude. All statistical analyses were performed in Matlab. We considered $p < 0.05$ to be the threshold for identifying significant regression relationships. We chose to perform unweighted regression, as opposed to weighted regression based on the standard error of sample measurements, for two reasons. First, a small number of sites with a large number of measurements, and therefore small standard error, had a disproportionate effect on weighted regression results. Second, in environmental research unweighted regression is frequently less biased than weighted regression (Fletcher and Dixon, 2012). Based on a test proposed by Fletcher and Dixon (2012), unweighted regression is appropriate for this dataset. We used analysis of covariance to test for significant differences between regression relationships.

To compare isotopic data (δ^2H-CH$_4$ and δ^{13}C-CH$_4$) between groups (i.e. latitudinal bands, ecosystem types, sample types) we used non-parametric statistical tests to test whether the groups were from different distributions. We used non-parametric tests because some sample groups were not normally distributed, as determined by a Shapiro-Wilk test (Shapiro and Wilk, 1965). For comparing differences between the distributions of two groups we used the Mann-Whitney U-test (Mann and Whitney, 1947), whereas when comparing differences between the distributions of more than two groups we used the Kruskal-Wallis H-test (Kruskal and Wallis, 1952), combined with Dunn's test to compare specific sample group pairs (Dunn, 1964). We considered $p < 0.05$ to be the threshold for identifying groups with significantly different distributions.

When comparing δ^{13}C-CH$_4$ by latitude and ecosystem we combined the data from this study with additional data from Sherwood et al. (2017) (32 additional sites) where δ^2H-CH$_4$ was not measured to make our dataset as representative as possible. To our knowledge this combined dataset is the largest available compiled dataset of freshwater δ^{13}C-CH$_4$, although there are many more δ^{13}C-CH$_4$ measurements that have not yet been aggregated. We did not include these

Peter Douglas 5/11/2021 1:55 PM

244 additional data when analysing differences by sample type, as sample type was not specified in the dataset of Sherwood
245 et al. (2017).

2.4 Estimation of global atmospheric CH_4 δ^2H and $\delta^{13}C$ source values

247 To better understand how latitudinal differences in wetland isotopic source signatures influence atmospheric δ^2H-CH_4
248 and $\delta^{13}C$-CH_4, we calculated a 'bottom-up' mixing model of δ^2H-CH_4 and $\delta^{13}C$-CH_4. For this calculation we ascribed all
249 CH_4 sources a flux (derived from Saunois et al., 2020; see details below) and a δ^2H and $\delta^{13}C$ value, and calculated the
250 global atmospheric source value using an isotopic mixing model. Because of non-linearity when calculating mixtures
251 using δ^2H values, we performed the mixing equation using isotopic ratios (see Sect. 2.1). The mixing equation is as
252 follows:

253 $$R_{mix} = f_1R_1 + f_2R_2 + ... + f_nR_n \qquad (4)$$

254 where f_n is the fractional flux for each source term (i.e. the ratio of the source flux to total flux), and R_n is the isotope
255 ratio for each source term.

256 Values for the flux, δ^2H, and $\delta^{13}C$ applied for each source term are shown in Table 1. We used bottom-up source
257 fluxes from Saunois et al. (2020) for the period 2008-2017. For categories other than wetlands, inland waters, and rice
258 paddies, we used global fluxes and isotope values, since geographically resolved isotopic source signature estimates are
259 not available. For these sources we used δ^2H and $\delta^{13}C$ values published by Sherwood et al. (2017), using the mean value
260 for each source term. For wetlands, inland waters, and rice paddies, we used geographically resolved (60-90 ºN; 30-60
261 ºN, 90º S-30ºN) fluxes derived from Saunois et al. (2019) for the period 2008-2017, and mean δ^2H-CH_4 for these
262 latitudinal bands from this study.

263 To calculate mean $\delta^{13}C$-CH_4 from wetlands, inland waters, and rice paddies for different latitudinal bands we
264 combined the data from this study along with additional data from Sherwood et al. (2017) (32 additional sites) to make
265 our estimated source signatures as representative as possible. To our knowledge this combined dataset is the largest
266 available compiled dataset of freshwater $\delta^{13}C$-CH_4 (See Sect. 2.3). Sites dominated by C_4 plants are notably
267 underrepresented in this combined dataset. In addition, the biomass burning dataset of Sherwood e al. (2017) contains
268 very few data from C_4 plant combustion. We performed a separate estimate of global source $\delta^{13}C$-CH_4 that attempted to
269 correct for these likely biases by making two adjustments: 1) using the estimated low-latitude wetland $\delta^{13}C$-CH_4
270 signature of Ganesan et al., (2018) (-56.7‰), which takes into account the predicted spatial distribution of C_4 plant
271 dominated wetlands; and 2) using the biomass burning $\delta^{13}C$-CH_4 signature of Schwietzke et al., (2016) (-22.3‰), which
272 is weighted by the predicted contribution from C_4 plant combustion. We did not attempt to take into account $\delta^{13}C$-CH_4
273 from ruminants feeding on C_4 plants. For the C_4 plant corrected $\delta^{13}C$-CH_4 estimate, we applied the same uncertainties that
274 are reported in Table 1.

Table 1: Estimates of source-specific fluxes, δ²H-CH4, and δ¹³C-CH4, and their uncertainties, used in mixing models and Monte Carlo analyses

Category	Flux (Tg/Yr)	Uncertainty	δ²H signature (‰, VSMOW)	Uncertainty	δ¹³C signature (‰, VPDB)	Uncertainty
Wetlands (<30N)	115	37.5	-301	15	-64.4	1.9
Wetlands (30-60N)	25	16.5	-324	14	-61.8	2.6
Wetlands (>60N)	9	8.0	-374	10	-62.7	3.0
Inland Waters (<30N)	80	39.4	-301	12	-57.1	3.0
Inland Waters (30-60N)	64	31.9	-308	18	-62.0	3.8
Inland Waters (>60N)	16	7.5	-347	9	-65.0	1.8
Geological (onshore)[a]	38	13.0	-189	44	-43.8	10.0
Wild animals[b]	2	2.0	-316	28	-65.4	3.5
Termites[c]	9	6.0	-343	50	-63.4	3.5
Permafrost soils (direct)[d]	1	0.5	-374	15	-64.4	1.7
Geological (offshore)[a]	7	7.0	-189	44	-43.8	10.0
Biogenic open and coastal[e]	6	3.0	-200	50	-80.0	20.0
Enteric fermentation and manure	111	5.0	-308	28	-65.4	3.5
Landfills and waste	65	4.5	-297	6	-56.0	4.9
Rice cultivation (<30N)	19	1.2	-324	8	-55.0	6.5
Rice cultivation (30-60N)	12	0.5	-325	8	-62.3	2.1
Coal mining	42	15.5	-232	5	-49.5	1.0
Oil and gas	79	13.0	-189	2	-43.8	0.5
Industry[f]	3	3.0	-189	2	-43.8	0.5
Transport[f]	4	4.0	-189	2	-43.8	0.5
Biomass burning[g]	17	6.0	-211	15	-26.2	2.0
Biofuel burning[g]	12	2.0	-211	15	-26.2	2.0

a-No specific isotopic measurements in the database (Sherwood et al., 2017). We applied the mean isotopic values for oil and gas, and applied the standard deviation of for oil and gas as the uncertainty

b-No specific isotopic measurements in database (Sherwood et al., 2017). We used the isotopic values and uncertainties from livestock

c- Only one δ²H measurement in database (Sherwood et al., 2017). We applied 50‰ as a conservative uncertainty estimate.

d- No specific isotopic measurement in database (Sherwood et al., 2017). We used the isotopic values and uncertainties for high-latitude wetlands

e- No specific isotopic measurements in database (Sherwood et al., 2017). We applied approximate isotopic values based on Whiticar, (1999), and conservatively large uncertainty estimates.

f-No specific isotopic measurements in database (Sherwood et al., 2017). We used the isotopic values and uncertainties for oil and gas.

g-We applied all isotopic measurements of biomass burning to both the biomass burning and biofuel burning categories. We did not correct for the relative proportion of C_3 and C_4 plant combustion sources (See Sect. 2.4)

278

Since fluxes from *other natural sources* are not differentiated for the period 2008-2017, we calculated the proportional contribution of each category of other natural sources for the period 2000-2009 (Saunois et al., 2020), and applied this to the total flux from other natural sources for 2008-2017. Inland waters and rice paddies do not have geographically resolved fluxes reported in Saunois et al. (2020). Therefore, we calculated the proportion of *other natural sources* attributed to inland waters from 2000-2009 (71%), and applied this proportion to the geographically resolved fluxes of *other natural sources*. Similarly, we calculated the proportion of *agricultural and waste sources* attributed to rice agriculture from 2008-2017 (15%), and applied this to the geographically resolved fluxes of *agricultural and waste fluxes*.

To estimate uncertainty in the modelled total source δ^2H and $\delta^{13}C$ values we conducted Monte Carlo analyses (Thompson et al., 1992). We first estimated the uncertainty for each flux, δ^2H, and $\delta^{13}C$ term. Flux uncertainties were defined as one half of the range of estimates provided by Saunois et al., (2020). For sources where fluxes were calculated as a proportion of a larger flux, we applied the same proportional calculation to uncertainty estimates. In cases where one half of the range of reported studies was larger than the flux estimate, we set the uncertainty to be equal to the flux estimate to avoid negative fluxes in the mixing model. Isotopic source signal uncertainties were defined as the 95% confidence interval of the mean value for a given source category. For some sources there is insufficient data to calculate a 95% confidence interval, and we applied a conservative estimate of uncertainty for these sources, as detailed in Table 1. Confidence intervals for fossil fuel isotopic source signatures do not take into account variation in emissions fluxes and isotopic values between regions or resource types (i.e. conventional vs. unconventional reservoirs). This variation is difficult to quantify with available datasets, but could imply additional uncertainty in global source signatures. We recalculated the δ^2H and $\delta^{13}C$ mixing models 10,000 times, each time sampling inputs from the uncertainty distribution for each variable. We assumed all uncertainties were normally distributed. We interpret the 2-sigma standard deviation of the resulting Monte Carlo distributions as an estimate of the uncertainty of our total atmospheric CH_4 source isotopic values. To examine how the Monte Carlo analyses were specifically influenced by uncertainty in isotopic source signatures vs. flux estimates, we conducted sensitivity tests where we set the uncertainty in either isotopic source signatures or flux estimates to zero. We also used the mixing model and Monte Carlo method to estimate the mean flux-weighted freshwater δ^2H-CH_4 and $\delta^{13}C$-CH_4, using only the inputs for freshwater environments (Wetlands, Inland Waters, and Rice Cultivation) from Table 1 (See Sect. 3.5)

3 Results and Discussion

3.1 Dataset distribution

The dataset is primarily concentrated in the northern hemisphere (Fig. 1A), but is distributed across a wide range of latitudes between 3ºS to 73ºN (Fig. 1C). The majority of sampled sites are from North America (Fig. 1B), but there are

Peter Douglas 5/11/2021 10:00 AM
Peter Douglas 5/11/2021 10:03 AM

Peter Douglas 5/11/2021 2:05 PM
Peter Douglas 5/11/2021 2:05 PM

314 numerous sites from Eurasia. A much smaller number of sites are from South America and Africa. We define three

315 latitudinal bands for describing geographic trends: low latitudes (3°S to 30°N); mid-latitudes (30° to 60°N); and high-

316 latitudes; (60° to 90°N). This definition was used primarily because it corresponds with a commonly applied geographic

317 classification of CH$_4$ fluxes (Saunois et al., 2020).
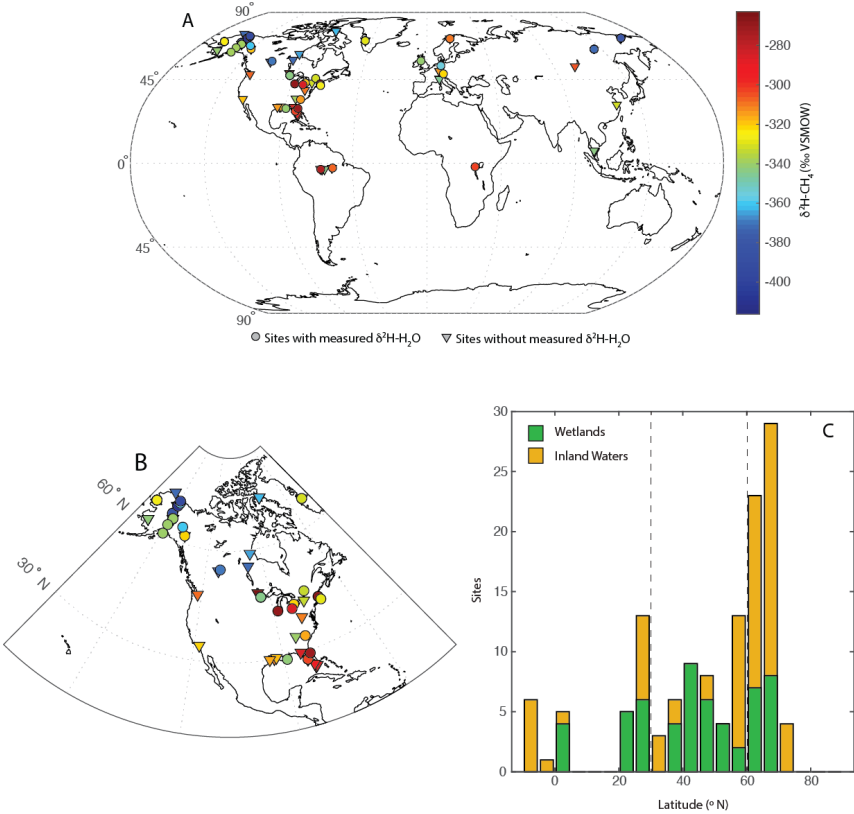
318

Figure 1: Distribution of sites shown; A) on a global map, with site mean CH$_4$-δ^{2}H values indicated in relation to a color bar. Sites with and without measured δ^{2}H-H$_2$O are differentiated; B) on a map of North America; and C) as a histogram of sites by latitude, differentiated between wetlands and inland waters. Dashed lines in (C) indicate divisions between low-latitude, mid-latitude, and high-latitude sites.

323 74 of 129 sites are classified as inland waters, primarily lakes (n = 66), with a smaller number from rivers (n =

324 8). To our knowledge, all of the inland water sites are natural ecosystems and do not include reservoirs. 55 sites are

330 classified as wetlands, including 16 bogs, 14 swamps and marshes, 12 fens, and 8 rice paddies. For the majority of sites

331 (n = 84) gas samples were measured, whereas studies at 36 sites measured dissolved CH_4 or diffusive fluxes.

3.2 Use of δ^2H_p as an estimator for freshwater $\delta^2H\text{-}H_2O$

333 As discussed in Sect. 2.2.3, we regressed annual and growing season δ^2H_p against measured $\delta^2H\text{-}H_2O$ to

334 determine which is a better estimator for sites where $\delta^2H\text{-}H_2O$ is not measured. We performed this analysis separately for

335 wetland and inland water environments because these broad environmental categories have distinct hydrological

336 characteristics. For all regression analyses we found strong correlations, with R^2 values between 0.82 to 0.88 (Fig. 2). For

337 wetlands, regression using annual δ^2H_p produces a slightly better fit, and also produces a slope within error of 1 (Fig 2A),

338 suggesting that variation in annual δ^2H_p scales proportionally with variation in measured $\delta^2H\text{-}H_2O$. However, the

339 intercept of this relationship was significantly greater than 0 (19±9 ‰). We interpret this intercept as indicating that

340 evaporative isotopic enrichment is generally important in controlling $\delta^2H\text{-}H_2O$ in wetlands. A slope slightly greater than

341 1 is also consistent with evaporative enrichment, since greater evaporation rates would be expected in low-latitude

342 environments with higher $\delta^2H\text{-}H_2O$. These results are consistent with detailed studies of wetland isotope hydrology that

343 indicate a major contribution from groundwater, with highly dampened seasonal variability relative to precipitation, but

344 also indicate evaporative enrichment of water isotopes in shallow soil water (Sprenger et al., 2017; David et al., 2018).

345 For inland waters, regression with growing season δ^2H_p produces a relationship that is within error of the 1:1

346 line (Fig. 2C), in contrast to annual δ^2H_p, which produces a flatter slope (Fig. 2D). We infer that seasonal differences in

347 δ^2H_p are important in determining $\delta^2H\text{-}H_2O$ in the inland water environments analyzed, especially at high latitudes,

348 implying that these environments generally have water residence times on subannual timescales. This finding is generally

349 consistent with evidence for seasonal variation in lake water isotopic compositions that is dependent on lake water

350 residence times (Tyler et al., 2007; Jonsson et al., 2009). Lake water residence times vary widely, primarily as a function

351 of lake size, but isotopic data implies that small lakes have water residence times of less than a year (Brooks et al., 2014),

352 resulting in seasonal isotopic variability (Jonsson et al., 2009). Isotopic enrichment of lake water is highly variable, but is

353 typically minor in humid and high-latitude regions (Jonsson et al., 2009; Brooks et al., 2014), which characterizes most

354 of our study sites.

355 Based on these results we, combine measured and estimated $\delta^2H\text{-}H_2O$ to determine a 'best-estimate' value for

356 each site, an approach similar to that of Waldron et al. (1999a). For sites with measured $\delta^2H\text{-}H_2O$ values we use that

357 value. For inland water sites without measured $\delta^2H\text{-}H_2O$ we use modeled growing season δ^2H_p since the regression of

358 this against measured $\delta^2H\text{-}H_2O$ is indistinguishable from the 1:1 line (Fig. 2D). For wetland sites without measured $\delta^2H\text{-}$

359 H_2O we estimate $\delta^2H\text{-}H_2O$ using the regression relationship with annual precipitation $\delta^2H\text{-}H_2O$ shown in Fig. 2A. The

360 root mean square errors (RMSE) of these relationships (16‰ for wetlands, 22‰ for inland waters) provide an estimate of

Peter Douglas 5/17/2021 3:18 PM

Peter Douglas 5/13/2021 12:32 PM

Peter Douglas 5/13/2021 12:31 PM

Peter Douglas 5/11/2021 10:53 AM

Peter Douglas 5/11/2021 2:08 PM

366   the uncertainty associated with estimating δ^2H-H_2O using δ^2H_p. Given the uncertainty associated with estimating δ^2H-

367   H_2O using δ^2H_p, for all analyses presented below that depend on δ^2H-H_2O values we also analyse the dataset only

368   including sites with measured δ^2H-H_2O.

369
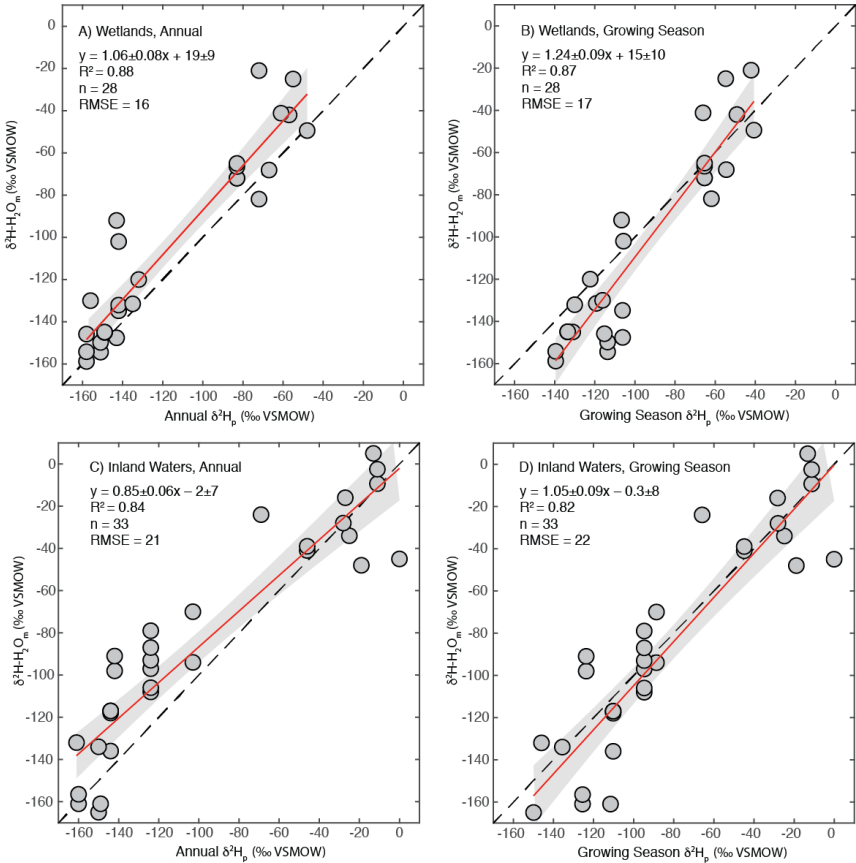
370   **Figure 2: Scatter plots of annual or growing season δ^2H_p vs. measured δ^2H-H_2O for wetland (A,B) and inland water (C,D)**
371   **sites. The red lines indicates the best fit, with a 95% confidence interval (gray envelopes), and the dashed black lines are the**
372   **1:1 relationship.**

373

374

3.3 Relationship between δ^2H-H$_2$O and δ^2H-CH$_4$

We carried out regression analyses of δ^2H-H$_2$O vs. δ^2H-CH$_4$, both using 'best-estimate' δ^2H-H$_2$O as described in sect. 3.2 (Fig. 3A), and only including sites with measured δ^2H-H$_2$O (Fig. 3B). In addition we analysed the relationship for all sites using annual (Fig. 3C) and growing season (Fig. 3D) δ^2H$_p$. Identifying the relationship between modelled δ^2H$_p$ and δ^2H-CH$_4$ is of value because this could be used to create gridded global predictions of δ^2H-CH$_4$ based on gridded datasets of δ^2H$_p$ (Bowen and Revenaugh, 2003), as well as to predict the distribution of δ^2H-CH$_4$ under past and future global climates using isotope enabled Earth system models (Zhu et al., 2017).

δ^2H-CH$_4$ is significantly positively correlated with δ^2H-H$_2$O when using all four methods of estimating δ^2H-H$_2$O (Fig. 3, Supplemental Table 2). This is the case when analysing all sites together, as well as when analysing wetlands and inland waters separately (Supplemental Table 2, Fig. 4). There is no significant difference in regression relationships, based on analysis of covariance, when δ^2H-CH$_4$ is regressed against best-estimate δ^2H-H$_2$O, measured δ^2H-H$_2$O, or modelled δ^2H$_p$, nor is there a major difference in R^2 values or RMSE (Supplemental Table S2). Regression with wetland sites consistently results in a higher R^2 values and lower RMSE than regression with inland water sites.

Given the similar results when regressing with estimated or measured δ^2H-H$_2$O, we infer that using either the 'best-estimate' δ^2H-H$_2$O or modelled δ^2H$_p$, instead of measured δ^2H-H$_2$O, to predict δ^2H-CH$_4$ does not result in substantial additional error. This implies that isotope-enabled Earth Systems models (ESMs) could be used to predict the distribution of freshwater δ^2H-CH$_4$ under past and future climates based on modeled δ^2H$_p$, although the substantial scatter in Figures 3C and D should be taken into account. The southern hemisphere is highly underrepresented in the δ^2H-CH$_4$ dataset. However, the mechanisms linking δ^2H-CH$_4$ with δ^2H-H$_2$O should not differ in the southern hemisphere, and we argue that the relationships observed in this study are suitable to predict southern hemisphere freshwater δ^2H-CH$_4$. The choice of predicting δ^2H-CH$_4$ using growing-season vs. annual precipitation δ^2H$_p$ could be important, with steeper slopes overall when regressing against growing season δ^2H$_p$. Based on our analysis in sect. 3.2, we suggest that annual δ^2H$_p$ may be more appropriate for estimating wetland δ^2H-CH$_4$, while growing season δ^2H$_p$ may be more appropriate for estimating inland water δ^2H-CH$_4$. Forthcoming research will combine gridded datasets of wetland distribution (Ganesan et al., 2018), modeled annual δ^2H$_p$ (Bowen and Revenaugh, 2003), and the regression relationships from this study to predict spatially-resolved wetland δ^2H-CH$_4$ at a global scale (Stell et al., in press).

411

Figure 3: Scatter plots of δ^2H-CH$_4$ vs. (A) best-estimate δ^2H-H$_2$O; (B) measured δ^2H-H$_2$O; (C) annual δ^2H$_p$; and (D) growing season δ^2H$_p$. Sites that were included in the analysis of Waldron et al. (1999a) are indicated. The regression relationship for the total dataset in each plot is shown by the red line, with its 95% confidence interval (grey envelope). The regression relationship and confidence interval for the dataset of Waldron et al., (1999a) is shown in blue. Uncertainties for reported regression relationships are standard errors.

Overall, our results are broadly consistent with those of Waldron et al., (1999a), and confirm the finding of that study that δ^2H-H$_2$O is the predominant predictor of global variation in δ^2H-CH$_4$. All of the regression slopes produced using our dataset are flatter than the regression relationship found by Waldron et al. (1999a) using a smaller dataset (0.68±0.1), although the slopes are not significantly different based on analysis of covariance. Based on this result we

infer that the true global relationship is likely flatter than that estimated by Waldron et al. (1999a). The difference between the regression relationships reported here and that of Waldron et al. (1999a) is largely a result of a much greater number of samples from the high latitudes (Fig. 1C), where δ^2H-H_2O values are typically lower. The small number of high-latitude sites sampled by Waldron et al. (1999a) are skewed towards the low end of the high-latitude δ^2H-CH_4 data from this study (Fig. 3). A similarly flatter slope (0.54±0.05) was found by Chanton et al. (2006) when combining a dataset of δ^2H-CH_4 from Alaskan wetlands, which are included in this study, with the dataset of Waldron et al. (1999a). Based on the range of R^2 values shown in Figure 3, we estimate that δ^2H-H_2O explains approximately 42% of variability in δ^2H-CH_4, implying substantial residual variability, with greater residual variability for inland water sites than for wetlands (Supplemental Table 2).

Given that δ^2H-H_2O is strongly influenced by latitude we examined whether δ^2H-CH_4 is also significantly correlated with latitude. There is indeed a significant, negative relationship between latitude and δ^2H-CH_4, indicating an approximate decrease of 0.9‰/° latitude (Fig. 4). The slope is significantly flatter than that for latitude vs. δ^2H-H_2O in this dataset (-2 ‰/° latitude), which is consistent with the inferred slope for δ^2H-H_2O vs. δ^2H-CH_4 (0.44 to 0.5). There is greater scatter in δ^2H-CH_4 at higher latitudes, especially for inland waters, but it is unclear if this is simply a result of a larger sample set or of differences in the underlying processes controlling δ^2H-CH_4. We discuss latitudinal differences in δ^2H-CH_4 in further detail in Sect. 3.5
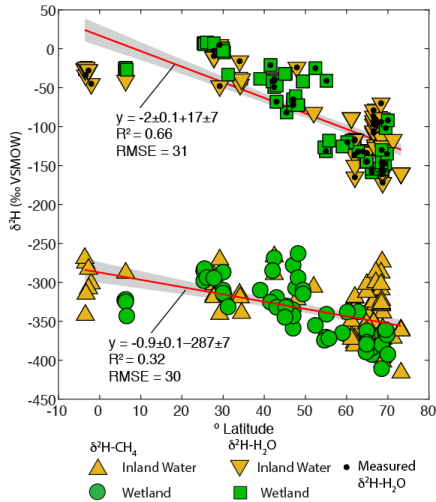
Figure 4: Scatter plots of δ^2H-CH_4 and best-estimate δ^2H-H_2O, vs. latitude (°N). Sites with measured δ^2H-H_2O are indicated. Envelopes indicate 95% confidence intervals for regression lines.

3.3.1 Comparison of δ^2H-H$_2$O vs δ^2H-CH$_4$ relationships between environmental and experimental studies

To further understand the processes controlling the observed freshwater δ^2H-H$_2$O vs. δ^2H-CH$_4$ relationships we compared them to results from pure culture and incubation experiments across a wide range of δ^2H-H$_2$O values (Fig. 5), focusing on regression against best-estimate δ^2H-H$_2$O. The regression slopes for both wetlands and inland waters (0.5 and 0.42) are within error of the 'in-vitro' relationship compiled by Waldron et al. (1999a) (0.44), based on laboratory incubations from three separate studies (Schoell, 1980;Sugimoto and Wada, 1995;Waldron et al., 1998). The intercept for the wetland and inland water regressions is higher than that for the 'in-vitro' relationship, although only the difference with inland waters is significant. In contrast, the regression slope for pure-culture acetoclastic methanogenesis experiments is much flatter (0.18 to 0.2) (Valentine et al., 2004b;Gruen et al., 2018), consistent with the prediction that one hydrogen atom is exchanged between water and the acetate methyl group during CH$_4$ formation (Pine and Barker, 1956;Whiticar, 1999). The large difference in intercept between the two acetate pure culture datasets is likely a function of differences in the δ^2H of acetate between the experiments, but could also be influenced by differences in kinetic isotope effects (Valentine et al., 2004b).

Pure culture hydrogenotrophic methanogenesis experiments (Gruen et al., 2018) yield a regression slope that is consistent with a constant α_H value, although α_H can clearly vary depending on experimental or envirornmental conditions (Valentine et al., 2004b;Stolper et al., 2015;Douglas et al., 2016). The wetland, inland water, and 'in-vitro' regression relationships are not consistent with a constant value of α_H (Fig. 5). Our comparison supports previous inferences that the in-vitro line of Waldron et al., (1999a) provides a good estimate of the slope of environmental δ^2H-H$_2$O vs. δ^2H-CH$_4$ relationships. This slope is likely controlled by the relative proportion of acetoclastic and hydrogenotrophic methanogenesis, the net kinetic isotope effect associated with these two methanogenic pathways, and variance in δ^2H of acetate (Waldron et al., 1998;Waldron et al., 1999a;Valentine et al., 2004a), but the relative importance of these variables remains uncertain.

In particular, the δ^2H of acetate methyl hydrogen is probably influenced by environmental δ^2H-H$_2$O, and therefore likely varies geographically as a function of δ^2H$_p$, as originally hypothesized by Waldron et al. (1999a). To our knowledge there are no measurements of acetate or acetate-methyl δ^2H from natural environments with which to test this hypothesis. In general, variability in the δ^2H of environmental organic molecules in lake sediments and wetlands, including fatty acids and cellulose, is largely controlled by δ^2H-H$_2$O (Huang et al., 2002;Sachse et al., 2012;Mora and Zanazzi, 2017), albeit with widely varying fractionation factors. The δ^2H of methoxyl groups in plants has also been shown to vary as a function of δ^2H-H$_2$O (Vigano et al., 2010). Furthermore, culture experiments with acetogenic bacteria imply that there is rapid isotopic exchange between H$_2$ and H$_2$O during chemoautotrophic acetogenesis (Valentine et al., 2004a), implying that the δ^2H of chemoautotrophic acetate is also partially controlled by environmental δ^2H-H$_2$O. Incubation experiments, such as those included in the 'in-vitro line' (Schoell, 1980;Sugimoto and Wada, 1995;Waldron

Peter Douglas 5/11/2021 11:44 AM

Peter Douglas 5/11/2021 2:15 PM

Peter Douglas 5/11/2021 2:15 PM

485   et al., 1998), probably contain acetate-δ^2H that varies as a function of ambient δ^2H-H_2O, given that the acetate in these

486   incubation experiments was actively produced by fermentation and/or acetogenesis during the course of the experiment.

487   This differs from pure cultures of methanogens, where acetate is provided in the culture medium and therefore does not

488   vary in its δ^2H value (Valentine et al., 2004b; Gruen et al., 2018).

489

490
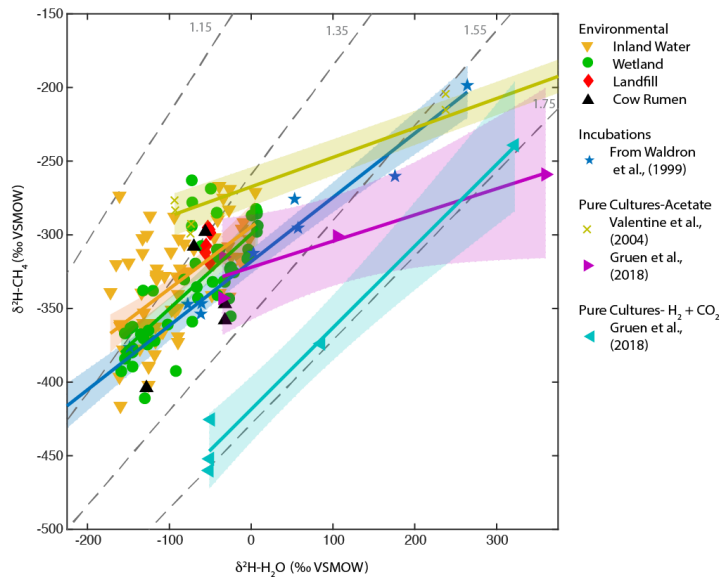
Figure 5: Scatter plots of δ^2H-CH_4 vs. δ^2H-H_2O for wetlands, inland waters, landfills, and cow rumen, compared with incubation and pure-culture experiments. Regression lines and confidence intervals corresponding to each dataset (except landfills and cow rumen) are shown. Dashed gray lines indicate constant values of α_H. Regression line statistics are listed in Supplemental Table S2. Plotted δ^2H-H_2O values are 'best-estimate' values for wetlands and inland waters, measured values for culture experiments, and a combination of measured values and annual δ^2H_p for landfills and cow rumen (See supplemental Table S3 for more details).

497   **3.4 Relationship of δ^2H-CH_4 with $\delta^{13}C$-CH_4, $\delta^{13}C$-CO_2, and α_C**

498   As shown in Fig. 3, there is a large amount of residual variability in δ^2H-CH_4 that is not explained by δ^2H-H_2O.

499   Several biogeochemical variables have been proposed to influence freshwater δ^2H-CH_4 independently of δ^2H-H_2O,

500   including the predominant biochemical pathway of methanogenesis (Whiticar et al., 1986;Whiticar, 1999;Chanton et al.,

501   2006), the extent of methane oxidation (Happell et al., 1994;Waldron et al., 1999a;Whiticar, 1999;Cadieux et al., 2016),

502   isotopic fractionation resulting from diffusive gas transport (Waldron et al., 1999a;Chanton, 2005), and differences in the

503   thermodynamic favorability or reversibility of methanogenesis (Valentine et al., 2004b;Stolper et al., 2015;Douglas et al.,

505   2016). These variables are also predicted to cause differences in $\delta^{13}C$-CH_4, $\delta^{13}C$-CO_2, and α_C. Therefore, we analysed co-
506   variation between δ^2H-$CH_{4,W0}$ (see definition in Sect. 2.2.3) and $\delta^{13}C$-CH_4, $\delta^{13}C$-CO_2, and α_C to see if it could partially
507   explain the residual variability in δ^2H-CH_4 (Fig. 6).

508   In order to facilitate interpretation of isotopic co-variation, we estimated approximate vectors of predicted
509   isotopic co-variation for the four variables being considered (Fig. 6). We emphasize that these vectors are uncertain, and
510   while they can be considered indicators for the sign of the slope of co-variation and the relative magnitude of expected
511   isotopic variability, they are not precise representations of the slope or intercept of isotopic co-variation. In reality,
512   isotopic co-variance associated with these processes likely varies depending on specific environmental conditions,
513   although the sign of co-variance should be consistent. The starting point for the vectors is arbitrarily set to typical
514   isotopic values for inferred acetoclastic methanogenesis in freshwater systems (Whiticar, 1999). We based the vectors for
515   differences in the dominant methanogenic pathway and methane oxidation on Figures 8, 5, and 10 in Whiticar (1999).
516   These figures are widely applied to interpret environmental isotopic data related to CH_4 cycling. However, we note that
517   both environmental and experimental research has questioned whether differences in the dominant methanogenic
518   pathway has an influence on δ^2H-CH_4 (Waldron et al., 1998;Waldron et al., 1999a). Differences in δ^2H-CH_4 between
519   hydrogenotrophic and acetoclastic methanogenesis are likely highly dependent on both the δ^2H of acetate and the carbon
520   and hydrogen kinetic isotope effects for both methanogenic pathways, both of which are poorly constrained in natural
521   environments and are likely to vary between sites (see Sect. 3.3.1). We did not differentiate between anaerobic and
522   aerobic methane oxidation, and the vectors shown are similar to experimental results for aerobic methane oxidation
523   (Wang et al., 2016).

524   The vector for isotopic fractionation related to gas-phase diffusion is based on the calculations of Chanton
525   (2005), and indicates isotopic change for residual gas following a diffusive loss. Gas-liquid diffusion is predicted to have
526   a much smaller isotopic effect (Chanton, 2005). The vector for differences in enzymatic reversibility are based on
527   experiments where CH_4 and CO_2 isotopic compositions were measured together with changes in methane production rate
528   or Gibbs free energy (Valentine et al., 2004b;Penning et al., 2005). We note that these studies did not measure δ^2H-CH_4
529   in the same experiments as $\delta^{13}C$-CH_4 or $\delta^{13}C$-CO_2, implying large uncertainty in the co-variance vectors. More detail on
530   the estimated vectors is provided in the Supplementary Text.
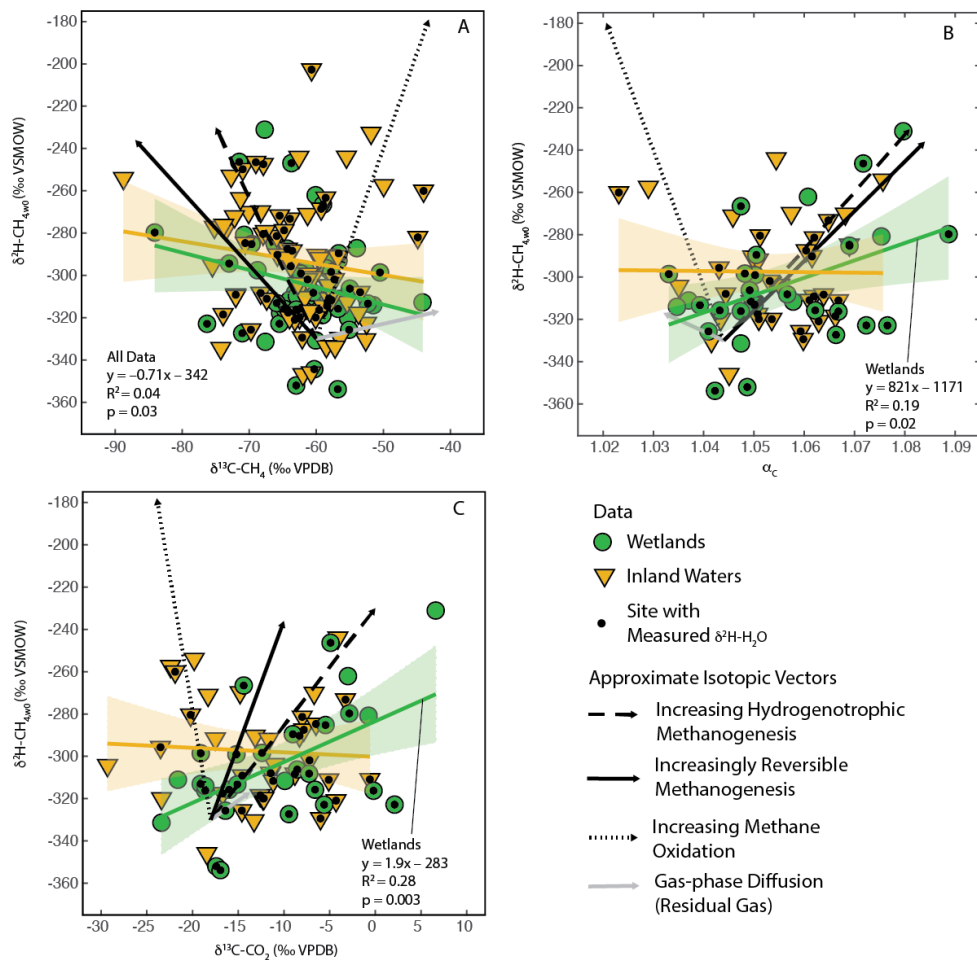
533
534 Figure 6: Scatter plots of δ^2H-CH$_{4,w0}$ vs. (A) δ^{13}C-CH$_4$, (B) α_c, and (C) δ^{13}C-CO$_2$. Approximate vectors for isotopic co-
535 variation related to four biogeochemical variables are shown. See details in Sect. 3.4 and the supplemental text. Regression
536 relationships are shown for wetland and inland water sites, with envelopes indicating 95% confidence intervals. Regression
537 statistics are shown here for relationships with significant correlations ($p < 0.05$). All regression statistics are detailed in
538 Supplemental Table S4.

We observe significant positive correlations between δ^2H-CH$_{4,W0}$, calculated using best estimate δ^2H-H$_2$O, and both δ^{13}C-CO$_2$, and α_C for wetland sites (Fig. 6B,C; Supplemental Table S4). We do not observe a significant correlation between these variables for inland water sites or for the dataset as a whole. We also observe a weak but significant negative correlation between δ^2H-CH$_{4,W0}$ and δ^{13}C-CH$_4$ for all sites, but not for data disaggregated into wetlands and inland water categories (Fig. 6A). The correlations shown in Figure 6 should be interpreted with caution, since repeating this analysis only using sites with measured δ^2H-H$_2$O does not result in any significant correlations (Supplemental Table S4). It is unclear whether this different result when using best-estimate or measured δ^2H-H$_2$O represents a bias related to estimating δ^2H-H$_2$O using δ^2H$_p$, or is an effect of the much smaller sample size for sites with δ^2H-H$_2$O measurements. If accurate, the observed significant positive correlations in Figures 6B and C suggest that residual variability in δ^2H-CH$_4$ in wetlands is more strongly controlled by biogeochemical variables related to methanogenesis, namely differences in methanogenic pathway or thermodynamic favorability, than post-production processes such as diffusive transport and CH$_4$ oxidation. For inland water sites our analysis suggests that no single biogeochemical variable has clear effect in controlling residual variability in δ^2H-CH$_4$.

Overall, our results are not consistent with arguments that residual variability in freshwater δ^2H-CH$_4$ is dominantly controlled by either differences in methanogenic pathway (Chanton et al., 2006), or post-production processes (Waldron et al., 1999a). Instead they highlight the combined influence of a complex set of variables and processes that are difficult to disentangle on an inter-site basis using δ^{13}C measurements alone. It is also important to note the likely importance of variables that could influence δ^{13}C-CH$_4$ or δ^{13}C-CO$_2$ but not necessarily affect δ^2H-CH$_4$, including variance in the δ^{13}C of soil or sediment organic matter (Conrad et al., 2011;Ganesan et al., 2018), diverse metabolic and environmental sources and sinks of CO$_2$ in aquatic environments, and Rayleigh fractionation associated with CH$_4$ carbon substrate depletion (Whiticar, 1999). Finally, the possible role of other carbon substrates, such as methanol, in CH$_4$ production could be important in controlling isotopic co-variation. Culture experiments suggest that CH$_4$ produced from methanol has low δ^{13}C and δ^2H values relative to other pathways (Krzycki et al., 1987;Penger et al., 2012;Gruen et al., 2018), although the importance of this difference in environmental CH$_4$ is unclear.

Further research examining intra-site isotopic co-variation, which largely avoids complications associated with estimating δ^2H-H$_2$O, would help to more clearly resolve the relative importance of these processes, and how they vary between environments. Expanded research using methyl fluoride to inhibit acetoclastic methanogenesis (Penning et al., 2005;Penning and Conrad, 2007;Conrad et al., 2011), with a particular focus on δ^2H-CH$_4$ measurements, would also help to clarify the importance of methanogenic pathway on isotopic co-variation. Finally, an expanded application of measurements of clumped isotopes, which have distinctive patterns of variation related to these processes (Douglas et al.,

588 2016; Douglas et al., 2017; Young et al., 2017; Douglas et al., 2020), would also be of value in determining their relative

589 importance in controlling δ^2H-CH$_4$ values in freshwater environments.

3.5 Differences in δ^2H-CH$_4$ and δ^{13}C-CH$_4$ by latitude

591 When analysing all sites together we found a significant difference in the distribution of δ^2H-CH$_4$ between high-

592 latitude sites (median: -351‰) and both low (median: -298‰) and mid-latitude sites (median: -320 ‰) (Fig. 7A).

593 However, we did not find a significant difference in the distribution of low- and mid-latitude sites. Similar differences

594 were found when the data were disaggregated into wetland and inland water sites. We also found that the distribution of

595 δ^{13}C-CH$_4$ for low latitude sites (median: -61.6‰) was significantly higher than for high latitude sites (median: −63.0‰),

596 but that mid-latitude sites (median: -60.3‰) were not significantly different from the other two latitudinal zones (Fig.

597 7B). The observed difference by latitudinal zone in δ^{13}C-CH$_4$ appears to be driven primarily by latitudinal differences

598 between inland water sites, where a similar pattern is found. In wetland sites we found no significant differences in the

599 distribution of δ^{13}C-CH$_4$ by latitude.
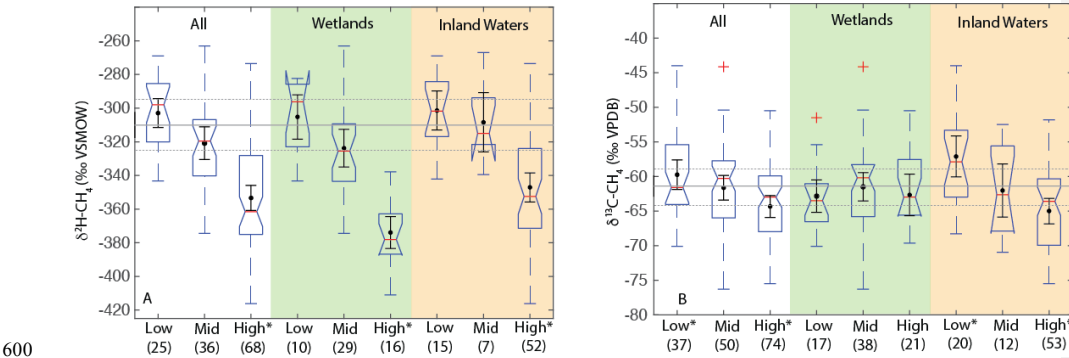
601 **Figure 7: Boxplots of (A) δ^2H-CH$_4$ and (B) δ^{13}C-CH$_4$ for sites differentiated by latitude, for all data, wetlands, and inland**
602 **waters. Numbers in parentheses indicate the number of sites for each category. Red lines indicate medians, boxes indicate 25th**
603 **and 75th percentiles, whiskers indicate 95th and 5th percentiles, and outliers are shown as red crosses. Notches indicate the 95%**
604 **confidence intervals of the median value; where notches overlap the edges of the box this indicates the median confidence**
605 **interval exceeds the 75th or 25th percentile. Black points and error bars indicate the category mean and 95% confidence**
606 **interval of the mean. Gray lines indicate the estimated flux-weighted mean values for global freshwater CH$_4$, and dashed lines**
607 **indicate the 95% confidence interval of this value. Asterisks in (A) indicate that high-latitude sites have significantly different**
608 **distributions from other latitudinal bands. Asterisks in (B) indicate groups that have significantly different distributions from**
609 **one another, within a specific environmental category. Two extremely low outliers (<-80‰; high latitude wetland and inland**
610 **water) are not shown in (B).**

611 Estimates of flux-weighted mean freshwater δ^2H-CH$_4$ and δ^{13}C-CH$_4$, calculated using the Monte Carlo approach

612 described in Sect. 2.4, are -310±15‰ (Fig. 7A) and -61.5±3‰ (Fig. 7B) respectively. Flux weighted mean values for

613 natural wetlands (not including inland waters or rice paddies) are -310±25‰ for δ^2H-CH$_4$ and -63.9±3.3‰ for δ^{13}C-CH$_4$.

615 Flux weighted mean values for inland waters are -309±31‰ for δ^2H-CH$_4$ and -60±5.7‰ for δ^{13}C-CH$_4$. As discussed in

616 Sect. 2.4 there are limited data in our dataset or that of Sherwood et al., (2017) from C$_4$ plant dominated wetlands, and

617 therefore our low-latitude and flux-weighted mean δ^{13}C-CH$_4$ values for wetlands are probably biased towards low values.

618 Differences in δ^2H-CH$_4$ by latitude has the potential to aid in geographic discrimination of freshwater methane

619 sources, both because it is based on a clear mechanistic linkage with δ^2H-H$_2$O (Figs. 3 and 4), and because geographic

620 variation in δ^2H-H$_2$O is relatively well understood (Bowen and Revenaugh, 2003;Bowen et al., 2005). However, recent

621 studies of atmospheric δ^2H-CH$_4$ variation have typically not accounted for geographic variation in source signals. As an

622 example, Rice et al., (2016) apply a constant δ^2H-CH$_4$ of -322‰ for both low-latitude (0-30º N) and high latitude (30-

623 90º N) wetland emissions. Based on our dataset this estimate is an inaccurate representation of wetland δ^2H-CH$_4$ for

624 either 0-30º N (mean: -305±13‰) or 30-90º N (mean: -345±11‰). Studies of ice core measurements have more

625 frequently differentiated freshwater δ^2H-CH$_4$ values as a function of latitude. For example, Bock et al., (2010)

626 differentiated δ^2H-CH$_4$ between tropical (-320‰) and boreal (-370‰) wetlands. This tropical wetland signature is

627 significantly lower than our estimate of low-latitude wetland δ^2H-CH$_4$, although the boreal wetland signature is similar to

628 our mean value for high-latitude wetlands (-374±10‰). Overall, our results imply that accounting for latitudinal variation

629 in freshwater δ^2H-CH$_4$, along with accurate latitudinal flux estimates, is important for developing accurate estimates of

630 global freshwater δ^2H-CH$_4$ source signatures.

631 Our analysis indicates significant differences in the distribution of freshwater δ^{13}C-CH$_4$ between the low- and

632 high-latitudes, but mid-latitude sites cannot be differentiated. Furthermore our results do not indicate significant

633 latitudinal differences in δ^{13}C-CH$_4$ for wetland sites in particular. This is in contrast to previous studies that have

634 inferred significant differences in wetland δ^{13}C-CH$_4$ by latitude (Bock et al., 2010;Rice et al., 2016;Ganesan et al., 2018).

635 An important caveat is that we have not analyzed a comprehensive dataset of freshwater δ^{13}C-CH$_4$, for which there are

636 much more published data than for δ^2H-CH$_4$, although our analysis does comprise the largest dataset of freshwater δ^{13}C-

637 CH$_4$ compiled to date (See Sect. 2.3). In addition, our analysis does not take into account the geographic distribution of

638 different ecosystem categories, although we do not find significant differences in δ^{13}C-CH$_4$ between ecosystem

639 categories (Fig. 8; Sect. 3.6). Low-latitude ecosystems dominated by C$_4$ plants are underrepresented both in our dataset

640 and that of Sherwood et al., (2017), and accounting for this would likely lead to a more enriched low-latitude wetland

641 δ^{13}C-CH$_4$. In contrast, high-latitude ecosystems, including bogs, are relatively well represented in these datasets (Fig. 8),

642 and we suggest that inferences of especially low δ^{13}C-CH$_4$ in high-latitude wetlands (Bock et al., 2010;Rice et al.,

643 2016;Ganesan et al., 2018) are not consistent with the compiled dataset of in-situ measurements. However, we note that

644 atmospheric estimates of high-latitude wetland δ^{13}C-CH$_4$ (~-68±4‰; Fisher et al., 2011) are lower than the median or

645 mean value shown in Figure 7B, and are in close agreement with the relatively low values predicted by (Ganesan et al.,

646 2018). Ombrotrophic and minerotrophic peatlands have distinctive δ^{13}C-CH$_4$ signatures (Bellisario et al., 1999;Bowes

Peter Douglas 5/11/2021 11:55 AM

Peter Douglas 5/11/2021 2:30 PM

Peter Douglas 5/11/2021 11:56 AM

Peter Douglas 5/11/2021 11:56 AM

653 and Hornibrook, 2006;Hornibrook, 2009), with lower signatures in ombrotrophic peatlands. We did not differentiate
654 peatlands by trophic status, and it is possible that the dataset of high-latitude wetland in-situ measurements is biased
655 towards minerotrophic peatlands with relatively high δ^{13}C-CH$_4$.

656 Latitudinal differences in δ^{13}C-CH$_4$ inferred by Ganesan et al. (2018) were based on two key mechanisms: (1)
657 differences in methanogenic pathway between different types of wetlands, especially between minerotrophic fens and
658 ombrotrophic bogs; and (2) differential inputs of organic matter from C$_3$ and C$_4$ plants. Because inferred latitudinal
659 differences in δ^{13}C-CH$_4$ and δ^2H-CH$_4$ are caused by different mechanisms, they could be highly complementary in
660 validating estimates of freshwater emissions by latitude. It is also important to note that previous assessments of
661 latitudinal differences in δ^{13}C-CH$_4$ did not include inland water environments. Our analysis suggests that latitudinal
662 variation in δ^{13}C-CH$_4$ in inland waters may be more pronounced than in wetlands, although the mechanisms causing this
663 difference will need to be elucidated with further study. A benefit of geographic discrimination based on δ^2H-CH$_4$ is that
664 the same causal mechanism applies to all freshwater emissions, including both wetlands and inland waters.

665 **3.5.1 Potential for geographic discrimination of other microbial methane sources based on δ^2H-CH$_4$**

666 We speculate that latitudinal differences in δ^2H-CH$_4$ should also be observed in other fluxes of microbial methane from
667 terrestrial environments, including enteric fermentation in livestock and wild animals, manure ponds, landfills, and
668 termites. This is because microbial methanogenesis in all of these environments will incorporate hydrogen from
669 environmental water, and therefore will be influenced by variation in precipitation δ^2H. There are limited data currently
670 available to test this prediction, but δ^2H-CH$_4$ data from cow rumen and landfills are available with either specified
671 locations or δ^2H-H$_2$O (Burke Jr, 1993;Levin et al., 1993;Liptay et al., 1998;Bilek et al., 2001;Wang et al., 2015;Teasdale
672 et al., 2019). These data plot in a range that is consistent with the δ^2H-CH$_4$ vs. δ^2H-H$_2$O relationships for freshwater CH$_4$
673 (Fig. 5). Landfill data are only available for a very small range of estimated δ^2H-H$_2$O, making it impossible to assess for
674 geographic variation currently. δ^2H-CH$_4$ data from cow rumen span a much wider range, and express substantial variation
675 that is independent of δ^2H-H$_2$O, but largely overlap measurements from freshwater environments. Based on these limited
676 data, variation observed in incubation studies that simulate landfill conditions (Schoell, 1980;Waldron et al., 1998), and
677 our understanding of the influence of δ^2H-H$_2$O on microbial δ^2H-CH$_4$ (Fig. 6), we suggest that both landfill and cow
678 rumen δ^2H-CH$_4$ likely vary geographically as a function of δ^2H-H$_2$O. If validated, this variation could also be used to
679 distinguish these CH$_4$ sources geographically. More data are clearly needed to test this conjecture, and it will also be
680 important to evaluate how closely annual or seasonal δ^2H$_p$ corresponds to environmental δ^2H-H$_2$O in both landfills and
681 cow rumen. Relatedly, the δ^2H of CH$_4$ emitted by biomass burning or directly by plants has also been shown to vary as a
682 function of δ^2H-H$_2$O (Vigano et al., 2010;Umezawa et al., 2011).

3.6 Differences in δ^2H-CH$_4$ and δ^{13}C-CH$_4$ by ecosystem

When comparing ecosystems, we analyze δ^2H-CH$_{4,W0}$ values to account for variability related to differences in δ^2H-H$_2$O. Ecosystem types are not evenly distributed by latitude, and therefore have different distributions of δ^2H-H$_2$O values. Our analysis does not find a significant difference in the distribution of δ^2H-CH$_{4,W0}$ between ecosystems, which could be partly a result of small sample sizes for most ecosystem categories (Fig. 8). Comparing the broader categories of inland waters and wetlands, we do observe a significant difference in δ^2H-CH$_{4,W0}$ distributions, with inland waters shifted towards higher values (median: -296‰) than wetlands (median: -311‰). We repeated this analysis only including sites with measured δ^2H-H$_2$O and found the same results in terms of category differences (Supplemental Figure S1). We did not observe any significant differences in δ^{13}C-CH$_4$ distributions between ecosystems, nor was there a significant difference in δ^{13}C-CH$_4$ distributions between inland waters and wetlands.

The significant difference in the distribution of δ^2H-CH$_{4,W0}$ between inland waters and wetlands is primarily a result of the difference in δ^2H-CH$_4$ between these environments in the high latitudes (Figs. 3, 4, and 7). We suggest this difference could be related to a greater overall prevalence of CH$_4$ oxidation in inland waters. As shown in Figure 6, the lack of positive co-variation between δ^2H-CH$_{4,W0}$ and δ^{13}C-CO$_2$, and α_C could be interpreted to support a greater role for CH$_4$ oxidation to control δ^2H-CH$_{4,W0}$ in inland waters relative to wetlands, although this result requires further validation. In lakes that undergo seasonal overturning and water column oxygenation there may be a greater overall effect of CH$_4$ oxidation than there are in wetlands typically. The absence of significant differences between ecosystems in terms of δ^{13}C-CH$_4$ (Fig. 8B) is in contrast to previous studies that have suggested that fens and bogs in particular have distinctive δ^{13}C-CH$_4$ (Ganesan et al., 2018). Bogs in particular have a very wide distribution of δ^{13}C-CH$_4$ that could represent differences between minerotrophic and ombrotrophic bogs (Hornibrook, 2009), which we did not differentiate in our dataset. This result should be interpreted with caution given that our dataset is not a comprehensive compilation of published δ^{13}C-CH$_4$ data, although it is the largest compiled dataset available (Sect. 2.3). We argue that inferred differences in δ^{13}C-CH$_4$ between wetland ecosystem categories should be further verified with more comprehensive data assimilation and additional measurements.

781

782 **Figure 8: Boxplots of (A) δ^2H-CH$_{4,w0}$ and (B) δ^{13}C-CH$_4$ for sites differentiated by ecosystem type. Numbers in parentheses**

783 **indicate the number of sites for each category. Boxplot parameters are as in Fig. 7. Black points and error bars indicate**

784 **the category mean and 95% confidence interval of the mean. Gray lines indicate the mean values across all categories and the**

785 **dashed lines indicate the 95% confidence interval of this value. Two extremely low outliers (<-80‰; lake and fen) are not**

786 **shown in (B). IW- Inland Waters; WL- Wetlands; S/M- Swamps and marshes. Asterisks in A indicate that inland waters and**

787 **wetlands have significantly different distributions.**

788 **3.7 Differences in δ^2H-CH$_4$ and δ^{13}C-CH$_4$ by sample type**

789 As with comparing ecosystems, when comparing sample types we analyze δ^2H-CH$_{4,W0}$ values to normalize for variability

790 related to differences in δ^2H-H$_2$O, since sample types are not distributed evenly by latitude. When comparing sample

791 types, dissolved CH$_4$ samples do not have a significantly different δ^2H-CH$_{4,W0}$ distribution for the dataset as a whole, nor

792 is there a significant difference between these groups in wetland sites (Fig. 9A). There is, however, a significant

793 difference in inland water sites, with dissolved CH$_4$ samples having a more enriched distribution (median: -270‰) vs.

794 gas samples (median: -302‰). We repeated this analysis only including sites with measured δ^2H-H$_2$O and found the

795 same results in terms of category differences (Supplemental Figure S2). We did not observe a significant difference in

796 the distribution of δ^{13}C between dissolved and gas-phase CH$_4$ samples, either for the dataset as a whole or when the

797 dataset was disaggregated into wetlands and inland waters (Fig. 9B).

798 We suggest that the higher δ^2H-CH$_{4,W0}$ in dissolved vs. gas samples for inland waters could be a result of

799 generally greater oxidation of dissolved CH$_4$ in inland water environments, potentially as a result of longer exposure to

800 aerobic conditions in lake or river water columns. This is in contrast to wetlands, where aerobic conditions are generally

801 limited to the uppermost layers of wetlands proximate to the water table. However, our dataset for inland water dissolved

804 CH$_4$ is quite small (n=9), and more data are needed to test this hypothesis. Furthermore, it is unclear why oxidation in

805 inland water dissolved CH$_4$ would be more strongly expressed in terms of δ^{2}H-CH$_{4,W0}$ (Fig. 9A) than δ^{13}C (Fig. 9B).

806   Overall, our data imply that isotopic differences between dissolved and gas phase methane are relatively minor

807 on a global basis, especially in wetlands. This result could imply that the relative balance of diffusive vs. ebullition gas

808 fluxes does not have a large effect on the isotopic composition of freshwater CH$_4$ emissions. However, our study does not

809 specifically account for isotopic fractionation occurring during diffusive or plant-mediated transport (Hornibrook, 2009),

810 and most of our dissolved sample data are of *in-situ* dissolved CH$_4$ and not diffusive fluxes. More isotopic data

811 specifically focused on diffusive methane emissions, for example using measurements of gas sampled from chambers,

812 would help to resolve this question, as would more comparisons of the isotopic composition of diffusive and ebullition

813 CH$_4$ emissions from the same ecosystem.

814
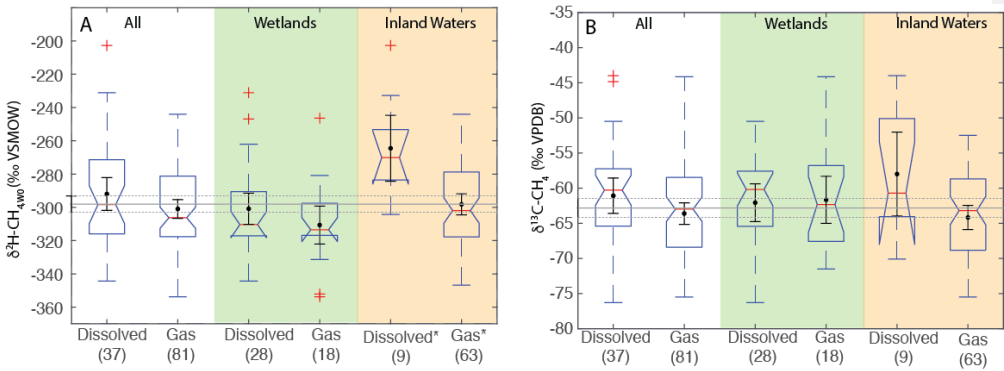
815 **Figure 9: Boxplots of (A) δ^{2}H-CH$_{4,w0}$ and (B) δ^{13}C-CH$_4$ for sites differentiated by sample type. Numbers in parentheses**

816 **indicate the number of sites for each category. Boxplot parameters are as in Fig. 7. Black points and error bars indicate the**

817 **category mean and 95% confidence interval of the mean. Gray lines indicate the mean values across all categories and the**

818 **dashed lines indicate the 95% confidence interval of this value. Two extremely low outliers (<-80‰; dissolved wetland and gas**

819 **inland water) are not shown in (B). Asterisks in A indicate that dissolved and gas-phase CH$_4$ samples from inland water sites**

820 **have significantly different distributions.**

821 **3.8 Estimates of global emissions source δ^{2}H-CH$_4$ and δ^{13}C-CH$_4$**

822 Our mixing model estimates a global source δ^{2}H-CH$_4$ of -278±15‰, and a global source δ^{13}C-CH$_4$ of -56.4±2.6‰ (Fig.

823 10). Monte Carlo sensitivity tests that only included uncertainty in either isotopic source signatures or flux estimates

824 suggest that larger uncertainty is associated with isotopic source signatures (12‰ for δ^{2}H; 2.2‰ for δ^{13}C) than with flux

825 estimates (8‰ for δ^{2}H; 1.4‰ for δ^{13}C). When correcting for wetland and biomass burning emissions from C$_4$ plant

826 ecosystems, as described in Section 2.4, our estimate of global source δ^{13}C-CH$_4$ increases to -55.2±2.6‰. Our estimate of

Peter Douglas 5/11/2021 12:13 PM

Peter Douglas 5/11/2021 2:37 PM

Peter Douglas 5/17/2021 3:48 PM

Peter Douglas 5/13/2021 1:43 PM

832   global source δ^2H-CH$_4$ is substantially higher than a previous bottom-up estimate using a similar approach (-295‰; Fig.

833   10) (Whiticar and Schaefer, 2007). This difference can be largely attributed to the application of more depleted δ^2H-CH$_4$

834   source signatures for tropical wetlands (-360 ‰), and to a lesser extent boreal wetlands (-380 ‰), by Whiticar and

835   Schaefer (2007).
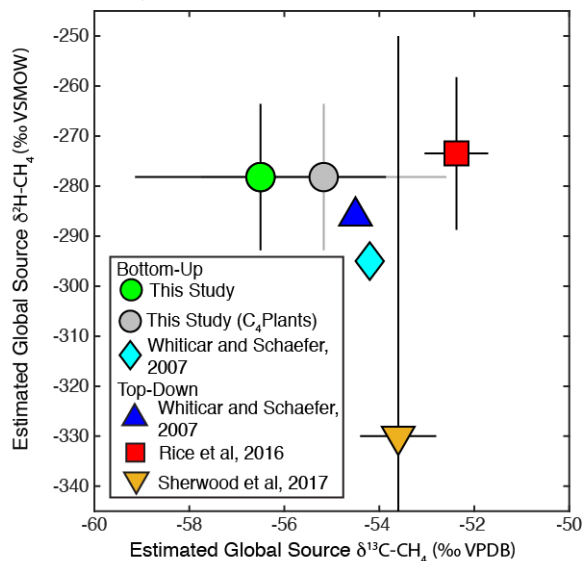
836

837   **Figure 10: Comparison of estimates of dual-isotope global source δ^2H-CH$_4$ and δ^{13}C-CH$_4$ from this and previous studies. Error**

838   **bars from this study indicate the 2σ standard deviation from Monte Carlo analysis. Gray dot and error bars indicate an**

839   **estimate corrected for the lack of data from wetlands and biomass burning in C$_4$ plant environments, as described in Sect. 2.4.**

840   **Error bars for Rice et al., (2016), indicate the range of values estimated in that study between 1977-2005. Error bars for**

841   **Sherwood et al., (2017) reflect the combined measurement uncertainty and uncertainty in sink fractionations reported in that**

842   **study. Whiticar and Schaefer (2007) did not provide uncertainties for their estimates.**

843   Our bottom-up estimate of global source δ^2H-CH$_4$ substantially overlaps the range of top-down estimates (-258

844   to -289‰) based on atmospheric δ^2H-CH$_4$ measurements from 1977-2005 and a box model of sink fluxes and kinetic

845   isotope effects (Rice et al., 2016) (Fig. 10). It is also within error of simpler top-down estimates calculated based on

846   mean atmospheric measurements and estimates of a constant sink fractionation factor (Whiticar and Schaefer,

847   2007;Sherwood et al., 2017). Sherwood et al., (2017) estimate a very wide range of possible global source δ^2H-CH$_4$

848   values based on a relatively large atmospheric sink fractionation with large uncertainty (-235±80‰). This range overlaps

849   with our bottom up estimate, although its mid-point is substantially lower than our estimate. We argue that the box-model

method used to account for sink fractionations applied by Rice et al. (2016) probably provides a more accurate representation of global-source isotopic composition than the other top-down estimates shown in Figure 10. The estimates of Rice et al. (2016) are also supported by the results of a global inversion model. Overall, the overlap between our bottom-up estimate of global source δ^2H-CH$_4$ with top-down estimates is encouraging, and suggests that the estimates of emission source δ^2H-CH$_4$ signatures applied in this study are reasonably accurate. However, as discussed below, there is still substantial scope to further constrain these estimates and to reduce uncertainty.

Our bottom-up estimate of global source δ^{13}C-CH$_4$ is lower than the other top-down and bottom-up estimates shown in Figure 10. As discussed above, there is likely a bias in our freshwater CH$_4$ isotopic database in that it includes very few wetland sites from C$_4$-plant dominated ecosystems. When correcting for this, as well as for CH$_4$ emissions from combustion of C$_4$ plants (Fig. 10), our estimate shifts to a more enriched value that is within uncertainty of other estimates. Clearly, accounting for the effect of C$_4$ plants in wetland and biomass burning CH$_4$ emissions, and potentially also in enteric fermentation emissions, is important for accurate estimates of global source δ^{13}C-CH$_4$. As discussed below, other sources of error in both isotopic source signatures and inventory-based flux estimates could also partially account for our relatively low global source δ^{13}C-CH$_4$ estimate. For example, variation in fossil fuel isotopic signatures between regions and resource types is potentially an additional source of uncertainty that is not accounted for in this estimate.

Previous studies have argued, on the basis of comparing atmospheric measurements and emissions source δ^{13}C-CH$_4$ signatures, that there are biases in global emissions inventories, specifically that fossil fuel emissions estimates are too low, and that either microbial emissions estimates are too high (Schwietzke et al., 2016), or that biomass burning estimates are too high (Worden et al., 2017). We argue that greater analysis of δ^2H-CH$_4$ measurements could be valuable for evaluating these and other emissions scenarios, as has been suggested previously (Rigby et al., 2012). This is especially true for determining the relative proportion of fossil fuel and microbial emissions, since these sources have widely differing δ^2H-CH$_4$ signatures (Table 1). Currently, atmospheric δ^2H-CH$_4$ measurements are not a routine component of CH$_4$ monitoring programs, but we argue that based on both their value in constraining emissions sources and sinks (Rigby et al., 2012), and the increasing practicality of high-frequency measurements (Chen et al., 2016;Röckmann et al., 2016;Yacovitch et al., 2020), that there should be a renewed focus on these measurements.

The uncertainty in our bottom-up estimates, the overall greater uncertainty associated with isotopic source signatures in our Monte Carlo calculations, and the apparent discrepancies for δ^{13}C-CH$_4$ shown in Figure 10, also imply that isotopic source signatures for specific sources could be greatly improved. As noted by Rigby et al. (2012), the impact of improved isotopic source signatures increases as measurement precision improves. We have discussed above the importance of increased data assimilation and measurements from tropical wetlands, with a particular focus on C$_4$ plant dominated ecosystems. Using the isotopic source signal uncertainties and emissions fluxes shown in Table 1, we identified the sources with the greatest flux-weighted uncertainty in isotopic signatures. Based on this analysis, the

893 greatest uncertainty for global source δ^2H-CH$_4$ estimates comes from source signatures for enteric fermentation and
894 manure, low-latitude wetlands, onshore geological emissions, low-latitude and mid-latitude inland waters, termites, and
895 landfills. We identified the same source categories as having the greatest flux-weighted uncertainty for δ^{13}C-CH$_4$, with
896 the exception of termites, but repeat the caveat that the underlying dataset is less comprehensive for δ^{13}C-CH$_4$. We argue
897 that these source categories should be considered priorities for future emissions source isotopic characterization through
898 data assimilation and additional measurements. As discussed in Sect. 3.5.1, evaluation of possible latitudinal variation in
899 enteric fermentation and landfill δ^2H-CH$_4$ is particularly promising.

5 Conclusions

901 Our analysis of an expanded isotopic dataset for freshwater CH$_4$ confirms the previous finding that δ^2H-H$_2$O is the
902 primary determinant of δ^2H-CH$_4$ on a global scale (Waldron et al., 1999a), but also finds that the slope of this
903 relationship is probably flatter than was inferred previously (Fig. 3). This flatter slope is primarily the result of the
904 inclusion of a much larger number of high-latitude sites with low δ^2H-H$_2$O our dataset. We find that the inferred
905 relationship between δ^2H-CH$_4$ and δ^2H-H$_2$O is not highly sensitive to whether measured δ^2H-H$_2$O, modeled δ^2H$_p$, or a
906 combination of the two (i.e. a best-estimate) is used to estimate δ^2H-H$_2$O. This implies that gridded datasets of δ^2H$_p$ or
907 isotope-enabled climate models could be used to predict the distribution of δ^2H-CH$_4$ in the present, as well as under past
908 and future climates. Our analysis also suggests that annual δ^2H$_p$ may be a better predictor for wetland δ^2H-CH$_4$, while
909 seasonal δ^2H$_p$ may be a better predictor of inland water δ^2H-CH$_4$. The slope of δ^2H-CH$_4$ vs. δ^2H-H$_2$O in both wetlands
910 and inland waters agrees well with that found in incubation experiments (Schoell, 1980;Sugimoto and Wada,
911 1995;Waldron et al., 1998;Waldron et al., 1999a), and we concur with previous inferences that this slope is partly
912 controlled by variation in the δ^2H of acetate as a function of δ^2H-H$_2$O (Waldron et al., 1999a). Analysis of co-variation of
913 δ^2H-CH$_{4,W0}$ with δ^{13}C-CH$_4$, δ^{13}C-CO$_2$, and α_C suggest that residual variation in δ^2H-CH$_4$ is influenced by a complex set
914 of biogeochemical variables, including both variable isotopic fractionation related to methanogenesis, and post-
915 production isotopic fractionation related to CH$_4$ oxidation and diffusive gas transport. A significant positive correlation
916 between δ^2H-CH$_{4,W0}$ and both δ^{13}C-CO$_2$, and α_C in wetlands suggests that hydrogen isotope fractionation related to
917 methanogenesis pathway or enzymatic reversibility may be more important in these environments, but this result is
918 dependent on the method used to estimate δ^2H-H$_2$O and requires further validation.

919 The dependence of δ^2H-CH$_4$ on δ^2H-H$_2$O leads to clear latitudinal differences in δ^2H-CH$_4$, with particularly low
920 values from high latitude sites (Fig. 4; Fig. 7A). The mechanism for latitudinal differences in δ^2H-CH$_4$ is distinct from
921 proposed mechanisms for latitudinal differences in δ^{13}C-CH$_4$ (Ganesan et al., 2018), implying that these two isotopic
922 tracers are complementary in differentiating geographic emissions sources. We estimate a global flux-weighted δ^2H-CH$_4$
923 signature from freshwater environments of -310±15‰, which is enriched relative to values used in previous source

Peter Douglas 5/11/2021 12:39 PM

Peter Douglas 5/11/2021 2:44 PM

Peter Douglas 5/13/2021 1:48 PM

Peter Douglas 5/13/2021 1:49 PM

Peter Douglas 5/11/2021 2:45 PM

apportionment studies (Rice et al., 2016;Bock et al., 2017). We observe a significantly higher δ^2H-CH$_{4,W0}$ distribution in inland waters relative to wetlands (Fig. 8A), which we suggest is a result of greater rates of CH$_4$ oxidation in inland waters. We do not find significant differences between more specific ecosystem categories, nor do we find significant differences in δ^2H-CH$_{4,W0}$ between sample types (Fig. 9A), with the exception of higher values in dissolved CH$_4$ relative to gas-phase CH$_4$ in inland water environments.

Our bottom-up estimate of the global δ^2H-CH$_4$ source signature, -278±15‰, is higher than previous bottom-up estimates (Whiticar and Schaefer, 2007), but is within the range of top-down estimates based on atmospheric measurements and modeled sink fractionations (Rice et al., 2016). In contrast, our bottom-up estimate of global δ^{13}C-CH$_4$, -56.4±2.6‰, is low relative to top-down estimates, which is partially explained by a lack of data from C$_4$ plant-dominated ecosystems in the freshwater CH$_4$ isotopic dataset. The agreement between bottom-up and top-down global δ^2H-CH$_4$ estimates suggests that our current understanding of δ^2H-CH$_4$ source signatures, when combined with inventory-based flux estimates (Saunois et al., 2020), is consistent with atmospheric measurements. This supports the argument that increased measurements and modeling of atmospheric δ^2H-CH$_4$ could help to constrain global CH$_4$ budgets (Rigby et al., 2012). However, there is clearly a need to better constrain source signatures for both δ^2H-CH$_4$ and δ^{13}C-CH$_4$, especially from low-latitude microbial sources.

Data Availability: The datasets used in this paper (Supplementary Tables 1-4) are publicly available: Douglas, Peter; Stratigopoulos, Emerald; Park, Jenny; Phan, Dawson (2020): Data for geographic variability in freshwater methane hydrogen isotope ratios and its implications for emissions source apportionment and microbial biogeochemistry. figshare. Dataset. https://doi.org/10.6084/m9.figshare.13194833.v2

Author Contribution: PMJD designed the project, assisted with compiling the data, analyzed the data, and wrote the manuscript; ES and JP compiled the data, and assisted with analyzing the data and editing the manuscript; DP developed code for mixing model and Monte Carlo calculations, and assisted with analyzing the data and editing the manuscript.

Competing Interests: The authors declare they have no competing interests.

Acknowledgments: We thank all of the researchers whose published data made this analysis possible (See Supplemental Table 1). We also thank Susan Waldron, Edward Hornibrook, and an anonymous reviewer for constructive feedback. This research was partially funded by McGill Science Undergraduate Research Awards to ES and JP and by NSERC Discovery Grant 2017-03902 to PMJD.

Peter Douglas 5/11/2021 12:40 PM

Peter Douglas 5/11/2021 2:46 PM

Peter Douglas 5/13/2021 1:50 PM

References

Alstad, K. P., and Whiticar, M. J.: Carbon and hydrogen isotope ratio characterization of methane dynamics for Fluxnet Peatland Ecosystems, Org Geochem, 42, 548-558, 2011.

Bastviken, D., Tranvik, L. J., Downing, J. A., Crill, P. M., and Enrich-Prast, A.: Freshwater methane emissions offset the continental carbon sink, Science, 331, 50-50, 2011.

Bellisario, L., Bubier, J., Moore, T., and Chanton, J.: Controls on CH4 emissions from a northern peatland, Global Biogeochem Cy, 13, 81-91, 1999.

Bergamaschi, P.: Seasonal variations of stable hydrogen and carbon isotope ratios in methane from a Chinese rice paddy, Journal of Geophysical Research: Atmospheres, 102, 25383-25393, 1997.

Bilek, R., Tyler, S., Kurihara, M., and Yagi, K.: Investigation of cattle methane production and emission over a 24-hour period using measurements of δ13C and δD of emitted CH4 and rumen water, Journal of Geophysical Research: Atmospheres, 106, 15405-15413, 2001.

Bock, M., Schmitt, J., Möller, L., Spahni, R., Blunier, T., and Fischer, H.: Hydrogen isotopes preclude marine hydrate CH4 emissions at the onset of Dansgaard-Oeschger events, Science, 328, 1686-1689, 2010.

Bock, M., Schmitt, J., Beck, J., Seth, B., Chappellaz, J., and Fischer, H.: Glacial/interglacial wetland, biomass burning, and geologic methane emissions constrained by dual stable isotopic CH4 ice core records, Proceedings of the National Academy of Sciences, 114, E5778-E5786, 2017.

Bouchard, F., Laurion, I., Preskienis, V., Fortier, D., Xu, X., and Whiticar, M.: Modern to millennium-old greenhouse gases emitted from ponds and lakes of the Eastern Canadian Arctic (Bylot Island, Nunavut), Biogeosciences, 12, 7279-7298, 2015.

Bowen, G. J., and Wilkinson, B.: Spatial distribution of δ18O in meteoric precipitation, Geology, 30, 315-318, 2002.

Bowen, G. J., and Revenaugh, J.: Interpolating the isotopic composition of modern meteoric precipitation, Water Resources Research, 39, 2003.

Bowen, G. J., Wassenaar, L. I., and Hobson, K. A.: Global application of stable hydrogen and oxygen isotopes to wildlife forensics, Oecologia, 143, 337-348, 2005.

Bowes, H. L., and Hornibrook, E. R.: Emission of highly 13C-depleted methane from an upland blanket mire, Geophys Res Lett, 33, 2006.

Brooks, J. R., Gibson, J. J., Birks, S. J., Weber, M. H., Rodecap, K. D., and Stoddard, J. L.: Stable isotope estimates of evaporation: inflow and water residence time for lakes across the United States as a tool for national lake water quality assessments, Limnol Oceanogr, 59, 2150-2165, 2014.

Brosius, L., Walter Anthony, K., Grosse, G., Chanton, J., Farquharson, L., Overduin, P. P., and Meyer, H.: Using the deuterium isotope composition of permafrost meltwater to constrain thermokarst lake contributions to atmospheric CH4 during the last deglaciation, Journal of Geophysical Research: Biogeosciences (2005–2012), 117, 2012.

Burke Jr, R.: SHALLOW AQUATIC SEDIMENTS, Bacterial Gas. Conference, Mila, September 25-26, 1989, 1992, 47,

Burke Jr, R. A., and Sackett, W. M.: Stable hydrogen and carbon isotopic compositions of biogenic methanes from several shallow aquatic environments, in, ACS Publications, 1986.

Burke Jr, R. A., Barber, T. R., and Sackett, W. M.: Methane flux and stable hydrogen and carbon isotope composition of sedimentary methane from the Florida Everglades, Global Biogeochem Cy, 2, 329-340, 1988.

Burke Jr, R. A., Barber, T. R., and Sackett, W. M.: Seasonal variations of stable hydrogen and carbon isotope ratios of methane in subtropical freshwater sediments, Global Biogeochem Cy, 6, 125-138, 1992.

Burke Jr, R. A.: Possible influence of hydrogen concentration on microbial methane stable hydrogen isotopic composition, Chemosphere, 26, 55-67, 1993.

Cadieux, S. B., White, J. R., Sauer, P. E., Peng, Y., Goldman, A. E., and Pratt, L. M.: Large fractionations of C and H isotopes related to methane oxidation in Arctic lakes, Geochim Cosmochim Ac, 187, 141-155, 2016.

Chanton, J., Whiting, G., Blair, N., Lindau, C., and Bollich, P.: Methane emission from rice: Stable isotopes, diurnal variations, and CO2 exchange, Global Biogeochem Cy, 11, 15-27, 1997.

Chanton, J. P.: The effect of gas transport on the isotope signature of methane in wetlands, Org Geochem, 36, 753-768, 2005.

Chanton, J. P., Fields, D., and Hines, M. E.: Controls on the hydrogen isotopic composition of biogenic methane from high-latitude terrestrial wetlands, Journal of Geophysical Research: Biogeosciences (2005–2012), 111, 2006.

Chasar, L., Chanton, J., Glaser, P. H., and Siegel, D.: Methane concentration and stable isotope distribution as evidence of rhizospheric processes: Comparison of a fen and bog in the Glacial Lake Agassiz Peatland complex, Annals of Botany, 86, 655-663, 2000.

Chen, Y., Lehmann, K. K., Peng, Y., Pratt, L., White, J., Cadieux, S., Sherwood Lollar, B., Lacrampe-Couloume, G., and Onstott, T. C.: Hydrogen Isotopic Composition of Arctic and Atmospheric CH4 Determined by a Portable Near-Infrared Cavity Ring-Down Spectrometer with a Cryogenic Pre-Concentrator, Astrobiology, 16, 787-797, 2016.

Conrad, R., Noll, M., Claus, P., Klose, M., Bastos, W., and Enrich-Prast, A.: Stable carbon isotope discrimination and microbiology of methane formation in tropical anoxic lake sediments, Biogeosciences, 8, 795, 2011.

Coplen, T. B.: Guidelines and recommended terms for expression of stable-isotope-ratio and gas-ratio measurement results, Rapid Commun Mass Sp, 25, 2538-2560, 2011.

David, K., Timms, W., Hughes, C. E., Crawford, J., and McGeeney, D.: Application of the pore water stable isotope method and hydrogeological approaches to characterise a wetland system, Hydrology and Earth System Sciences, 22, 6023-6041, 2018.

Douglas, P.M.J., Stolper, D., Smith, D., Walter Anthony, K., Paull, C., Dallimore, S., Wik, M., Crill, P., Winterdahl, M., Eiler, J., and Sessions, A. L.: Diverse origins of Arctic and Subarctic methane point source emissions identified with multiply-substituted isotopologues, Geochim Cosmochim Ac, 188, 163-188, 2016.

Douglas, P.M.J., Stolper, D. A., Eiler, J. M., Sessions, A. L., Lawson, M., Shuai, Y., Bishop, A., Podlaha, O. G., Ferreira, A. A., and Neto, E. V. S.: Methane clumped isotopes: progress and potential for a new isotopic tracer, Org Geochem, 113, 262-282, 2017.

Douglas, P.M.J., Gonzalez Moguel, R., Walter Anthony, K. M., Wik, M., Crill, P. M., Dawson, K. S., Smith, D. A., Yanay, E., Lloyd, M. K., and Stolper, D. A.: Clumped isotopes link older carbon substrates with slower rates of methanogenesis in northern lakes, Geophys Res Lett, 47, e2019GL086756, 2020.

Douglas, P.M.J.; Stratigopoulos, E.; Park, J.; Phan, D.; Data for geographic variability in freshwater methane hydrogen isotope ratios and its implications for emissions source apportionment and microbial biogeochemistry. figshare. https://doi.org/10.6084/m9.figshare.13194833.v2

Drevon, D., Fursa, S. R., and Malcolm, A. L.: Intercoder reliability and validity of WebPlotDigitizer in extracting graphed data, Behavior modification, 41, 323-339, 2017.

Dunn, O. J.: Multiple comparisons using rank sums, Technometrics, 6, 241-252, 1964.

Fisher, R. E., Sriskantharajah, S., Lowry, D., Lanoisellé, M., Fowler, C., James, R., Hermansen, O., Lund Myhre, C., Stohl, A., Greinert, J., and Nisbet, E. G.: Arctic methane sources: Isotopic evidence for atmospheric inputs, Geophys Res Lett, 38, L21803, 2011.

Fletcher, D., and Dixon, P. M.: Modelling data from different sites, times or studies: weighted vs. unweighted regression, Methods in Ecology and Evolution, 3, 168-176, 2012.

Ganesan, A., Stell, A., Gedney, N., Comyn-Platt, E., Hayman, G., Rigby, M., Poulter, B., and Hornibrook, E.: Spatially resolved isotopic source signatures of wetland methane emissions, Geophys Res Lett, 45, 3737-3745, 2018.

Gruen, D. S., Wang, D. T., Könneke, M., Topçuoğlu, B. D., Stewart, L. C., Goldhammer, T., Holden, J. F., Hinrichs, K.-U., and Ono, S.: Experimental investigation on the controls of clumped isotopologue and hydrogen isotope ratios in microbial methane, Geochim Cosmochim Ac, 237, 339-356, 2018.

Happell, J. D., Chanton, J. P., Whiting, G. J., and Showers, W. J.: Stable isotopes as tracers of methane dynamics in Everglades marshes with and without active populations of methane oxidizing bacteria, Journal of Geophysical Research: Atmospheres, 98, 14771-14782, 1993.

Happell, J. D., Chanton, J. P., and Showers, W. S.: The influence of methane oxidation on the stable isotopic composition of methane emitted from Florida swamp forests, Geochim Cosmochim Ac, 58, 4377-4388, 1994.

Hornibrook, E. R., Longstaffe, F. J., and Fyfe, W. S.: Spatial distribution of microbial methane production pathways in temperate zone wetland soils: stable carbon and hydrogen isotope evidence, Geochim Cosmochim Ac, 61, 745-753, 1997.

Peter Douglas 5/11/2021 12:42 PM

Peter Douglas 5/11/2021 12:42 PM

Peter Douglas 5/17/2021 4:00 PM

Peter Douglas 5/17/2021 4:00 PM

Peter Douglas 5/17/2021 3:59 PM

Hornibrook, E. R.: The stable carbon isotope composition of methane produced and emitted from northern peatlands, Baird, A., Belyea, L., Comas, X., Reeve, A., and Slater, L., American Geophysical Union, Geophysical Monograph Series, 184, 187-203, 2009.

Huang, Y., Shuman, B., Wang, Y., and Webb III, T.: Hydrogen isotope ratios of palmitic acid in lacustrine sediments record late Quaternary climate variations, Geology, 30, 1103-1106, 2002.

Jonsson, C. E., Leng, M. J., Rosqvist, G. C., Seibert, J., and Arrowsmith, C.: Stable oxygen and hydrogen isotopes in sub-Arctic lake waters from northern Sweden, J Hydrol, 376, 143-151, 2009.

Kai, F. M., Tyler, S. C., Randerson, J. T., and Blake, D. R.: Reduced methane growth rate explained by decreased Northern Hemisphere microbial sources, Nature, 476, 194-197, 2011.

Kruskal, W. H., and Wallis, W. A.: Use of ranks in one-criterion variance analysis, Journal of the American statistical Association, 47, 583-621, 1952.

Krzycki, J., Kenealy, W., DeNiro, M., and Zeikus, J.: Stable carbon isotope fractionation by Methanosarcina barkeri during methanogenesis from acetate, methanol, or carbon dioxide-hydrogen, Applied and Environmental Microbiology, 53, 2597-2599, 1987.

Lansdown, J., Quay, P., and King, S.: CH4 production via CO2 reduction in a temperate bog: A source of 13C-depIeted CH4, Geochim Cosmochim Ac, 56, 3493-3503, 1992.

Lansdown, J. M.: The carbon and hydrogen stable isotope composition of methane released from natural wetlands and ruminants, PhD Dissertation, University of Washington, 1992.

Lecher, A. L., Chuang, P. C., Singleton, M., and Paytan, A.: Sources of methane to an Arctic lake in Alaska: An isotopic investigation, Journal of Geophysical Research: Biogeosciences, 122, 753-766, 2017.

Levin, I., Bergamaschi, P., Dörr, H., and Trapp, D.: Stable isotopic signature of methane from major sources in Germany, Chemosphere, 26, 161-177, 1993.

Liptay, K., Chanton, J., Czepiel, P., and Mosher, B.: Use of stable isotopes to determine methane oxidation in landfill cover soils, Journal of Geophysical Research: Atmospheres, 103, 8243-8250, 1998.

Mann, H. B., and Whitney, D. R.: On a test of whether one of two random variables is stochastically larger than the other, The annals of mathematical statistics, 50-60, 1947.

Marik, T., Fischer, H., Conen, F., and Smith, K.: Seasonal variations in stable carbon and hydrogen isotope ratios in methane from rice fields, Global Biogeochem Cy, 16, 41-41-41-11, 2002.

Martens, C. S., Kelley, C. A., Chanton, J. P., and Showers, W. J.: Carbon and hydrogen isotopic characterization of methane from wetlands and lakes of the Yukon-Kuskokwim delta, western Alaska, Journal of Geophysical Research: Atmospheres (1984–2012), 97, 16689-16701, 1992.

Miles, N. L., Martins, D. K., Richardson, S. J., Rella, C. W., Arata, C., Lauvaux, T., Davis, K. J., Barkley, Z. R., McKain, K., and Sweeney, C.: Calibration and field testing of cavity ring-down laser spectrometers measuring CH 4, CO 2, and δ 13 CH 4 deployed on towers in the Marcellus Shale region, Atmospheric Measurement Techniques, 11, 1273-1295, 2018.

Mischler, J. A., Sowers, T. A., Alley, R. B., Battle, M., McConnell, J., Mitchell, L., Popp, T., Sofen, E., and Spencer, M.: Carbon and hydrogen isotopic composition of methane over the last 1000 years, Global Biogeochem Cy, 23, 2009.

Mora, G., and Zanazzi, A.: Hydrogen isotope ratios of moss cellulose and source water in wetlands of Lake Superior, United States reveal their potential for quantitative paleoclimatic reconstructions, Chem Geol, 468, 75-83, 2017.

Nakagawa, F., Yoshida, N., Sugimoto, A., Wada, E., Yoshioka, T., Ueda, S., and Vijarnsorn, P.: Stable isotope and radiocarbon compositions of methane emitted from tropical rice paddies and swamps in Southern Thailand, Biogeochemistry, 61, 1-19, 2002a.

Nakagawa, F., Yoshida, N., Nojiri, Y., and Makarov, V.: Production of methane from alasses in eastern Siberia: Implications from its 14C and stable isotopic compositions, Global Biogeochem Cy, 16, 14-11-14-15, 2002b.

Nisbet, E., Dlugokencky, E., Manning, M., Lowry, D., Fisher, R., France, J., Michel, S., Miller, J., White, J., and Vaughn, B.: Rising atmospheric methane: 2007–2014 growth and isotopic shift, Global Biogeochem Cy, 30, 1356-1370, 2016.

Nisbet, E. G., Manning, M., Dlugokencky, E., Fisher, R., Lowry, D., Michel, S., Myhre, C. L., Platt, S. M., Allen, G., and Bousquet, P.: Very strong atmospheric methane growth in the 4 years 2014–2017: Implications for the Paris Agreement, Global Biogeochem Cy, 33, 318-342, 2019.

Penger, J., Conrad, R., and Blaser, M.: Stable carbon isotope fractionation by methylotrophic methanogenic archaea, Applied and environmental microbiology, 78, 7596-7602, 2012.

Penning, H., Plugge, C. M., Galand, P. E., and Conrad, R.: Variation of carbon isotope fractionation in hydrogenotrophic methanogenic microbial cultures and environmental samples at different energy status, Global Change Biol, 11, 2103-2113, 2005.

Penning, H., and Conrad, R.: Quantification of carbon flow from stable isotope fractionation in rice field soils with different organic matter content, Org Geochem, 38, 2058-2069, 2007.

Pine, M. J., and Barker, H.: Studies on the methane fermentation XII.: The pathway of hydrogen in the acetate fermentation, Journal of Bacteriology, 71, 644-648, 1956.

Pison, I., Ringeval, B., Bousquet, P., Prigent, C., and Papa, F.: Stable atmospheric methane in the 2000s: key-role of emissions from natural wetlands, 2013.

Popp, T. J., Chanton, J. P., Whiting, G. J., and Grant, N.: Methane stable isotope distribution at a Carex dominated fen in north central Alberta, Global Biogeochem Cy, 13, 1063-1077, 1999.

Rice, A. L., Butenhoff, C. L., Teama, D. G., Röger, F. H., Khalil, M. A. K., and Rasmussen, R. A.: Atmospheric methane isotopic record favors fossil sources flat in 1980s and 1990s with recent increase, Proceedings of the National Academy of Sciences, 113, 10791-10796, 2016.

Rigby, M., Manning, A., and Prinn, R.: The value of high-frequency, high-precision methane isotopologue measurements for source and sink estimation, Journal of Geophysical Research: Atmospheres, 117, 2012.

Röckmann, T., Eyer, S., Van Der Veen, C., Popa, M. E., Tuzson, B., Monteil, G., Houweling, S., Harris, E., Brunner, D., and Fischer, H.: In situ observations of the isotopic composition of methane at the Cabauw tall tower site, Atmos. Chem. Phys., 16, 10469-10487, 2016.

Rozanski, K., Araguás-Araguás, L., and Gonfiantini, R.: Isotopic patterns in modern global precipitation, Geophysical Monograph Series, 78, 1-36, 1993.

Sachse, D., Billault, I., Bowen, G. J., Chikaraishi, Y., Dawson, T. E., Feakins, S. J., Freeman, K. H., Magill, C. R., McInerney, F. A., and van der Meer, M. T. J.: Molecular paleohydrology: Interpreting the hydrogen-isotopic composition of lipid biomarkers from photosynthesizing organisms, Annual Review of Earth and Planetary Sciences, 40, 221-249, 2012.

Sakagami, H., Takahashi, N., Hachikubo, A., Minami, H., Yamashita, S., Shoji, H., Khlystov, O., Kalmychkov, G., Grachev, M., and De Batist, M.: Molecular and isotopic composition of hydrate-bound and dissolved gases in the southern basin of Lake Baikal, based on an improved headspace gas method, Geo-Mar Lett, 32, 465-472, 2012.

Saunois, M., Stavert, A. R., Poulter, B., Bousquet, P., Canadell, J. G., Jackson, R. B., Raymond, P. A., Dlugokencky, E. J., Houweling, S., and Patra, P. K.: The global methane budget 2000–2017, Earth System Science Data, 12, 1561-1623, 2020.

Schaefer, H., Fletcher, S. E. M., Veidt, C., Lassey, K. R., Brailsford, G. W., Bromley, T. M., Dlugokencky, E. J., Michel, S. E., Miller, J. B., and Levin, I.: A 21st-century shift from fossil-fuel to biogenic methane emissions indicated by 13CH4, Science, 352, 80-84, 2016.

Schoell, M.: The hydrogen and carbon isotopic composition of methane from natural gases of various origins, Geochim Cosmochim Ac, 44, 649-661, 1980.

Schoell, M.: Genetic characterization of natural gases, AAPG bulletin, 67, 2225-2238, 1983.

Schwietzke, S., Sherwood, O. A., Bruhwiler, L. M., Miller, J. B., Etiope, G., Dlugokencky, E. J., Michel, S. E., Arling, V. A., Vaughn, B. H., and White, J. W.: Upward revision of global fossil fuel methane emissions based on isotope database, Nature, 538, 88-91, 2016.

Shapiro, S. S., and Wilk, M. B.: An analysis of variance test for normality (complete samples), Biometrika, 52, 591-611, 1965.

Sherwood, O. A., Schwietzke, S., Arling, V. A., and Etiope, G.: Global inventory of gas geochemistry data from fossil fuel, microbial and burning sources, version 2017, Earth System Science Data, 9, 2017.

Shoemaker, J., Varner, R., and Schrag, D.: Characterization of subsurface methane production and release over 3 years at a New Hampshire wetland, Geochim Cosmochim Ac, 91, 120-139, 2012.

Sprenger, M., Tetzlaff, D., Tunaley, C., Dick, J., and Soulsby, C.: Evaporation fractionation in a peatland drainage network affects stream water isotope composition, Water Resources Research, 53, 851-866, 2017.

1178 Stell, A. C., Douglas, P.M.J., Rigby, M., and Ganesan, A.L.: The impact of spatially varying wetland source signatures
1179 on the atmospheric variability of δD-CH$_4$, Philosophical Transactions of the Royal Society A. Accepted article in press,
1180 2021.
1181 Stolper, D., Martini, A., Clog, M., Douglas, P., Shusta, S., Valentine, D., Sessions, A., and Eiler, J.: Distinguishing and
1182 understanding thermogenic and biogenic sources of methane using multiply substituted isotopologues, Geochim
1183 Cosmochim Ac, 161, 219-247, 2015.
1184 Sugimoto, A., and Wada, E.: Hydrogen isotopic composition of bacterial methane: CO_2/H_2 reduction and acetate
1185 fermentation, Geochim Cosmochim Ac, 59, 1329-1337, 1995.
1186 Teasdale, C. J., Hall, J. A., Martin, J. P., and Manning, D. A.: Discriminating methane sources in ground gas emissions in
1187 NW England, Quarterly Journal of Engineering Geology and Hydrogeology, 52, 110-122, 2019.
1188 Thompson, H. A., White, J. R., Pratt, L. M., and Sauer, P. E.: Spatial variation in flux, δ 13 C and δ 2 H of methane in a
1189 small Arctic lake with fringing wetland in western Greenland, Biogeochemistry, 131, 17-33, 2016.
1190 Thompson, K. M., Burmaster, D. E., and Crouch3, E. A.: Monte Carlo techniques for quantitative uncertainty analysis in
1191 public health risk assessments, Risk Analysis, 12, 53-63, 1992.
1192 Thompson, R. L., Nisbet, E., Pisso, I., Stohl, A., Blake, D., Dlugokencky, E., Helmig, D., and White, J.: Variability in
1193 atmospheric methane from fossil fuel and microbial sources over the last three decades, Geophys Res Lett, 45, 11,499-
1194 411,508, 2018.
1195 Turner, A. J., Frankenberg, C., and Kort, E. A.: Interpreting contemporary trends in atmospheric methane, Proceedings of
1196 the National Academy of Sciences, 116, 2805-2813, 2019.
1197 Tyler, J. J., Leng, M. J., and Arrowsmith, C.: Seasonality and the isotope hydrology of Lochnagar, a Scottish mountain
1198 lake: implications for palaeoclimate research, The Holocene, 17, 717-727, 2007.
1199 Tyler, S., Bilek, R., Sass, R., and Fisher, F.: Methane oxidation and pathways of production in a Texas paddy field
1200 deduced from measurements of flux, δl3C, and δD of CH4, Global Biogeochem Cy, 11, 323-348, 1997.
1201 Umezawa, T., Aoki, S., Kim, Y., Morimoto, S., and Nakazawa, T.: Carbon and hydrogen stable isotopic ratios of
1202 methane emitted from wetlands and wildfires in Alaska: Aircraft observations and bonfire experiments, Journal of
1203 Geophysical Research: Atmospheres, 116, 2011.
1204 Valentine, D., Sessions, A., Tyler, S., and Chidthaisong, A.: Hydrogen isotope fractionation during H2/CO2
1205 acetogenesis: hydrogen utilization efficiency and the origin of lipid-bound hydrogen, Geobiology, 2, 179-188, 2004a.
1206 Valentine, D. L., Chidthaisong, A., Rice, A., Reeburgh, W. S., and Tyler, S. C.: Carbon and hydrogen isotope
1207 fractionation by moderately thermophilic methanogens, Geochim Cosmochim Ac, 68, 1571-1590, 2004b.
1208 Vigano, I., Holzinger, R., Keppler, F., Greule, M., Brand, W. A., Geilmann, H., Van Weelden, H., and Röckmann, T.:
1209 Water drives the deuterium content of the methane emitted from plants, Geochim Cosmochim Ac, 74, 3865-3873, 2010.
1210 Wahlen, M.: Carbon dioxide, carbon monoxide and methane in the atmosphere: abundance and isotopic composition,
1211 Stable isotopes in ecology and environmental science, 93-113, 1994.
1212 Waldron, S., Watson-Craik, I. A., Hall, A. J., and Fallick, A. E.: The carbon and hydrogen stable isotope composition of
1213 bacteriogenic methane: a laboratory study using a landfill inoculum, Geomicrobiology Journal, 15, 157-169, 1998.
1214 Waldron, S., Lansdown, J., Scott, E., Fallick, A., and Hall, A.: The global influence of the hydrogen iostope composition
1215 of water on that of bacteriogenic methane from shallow freshwater environments, Geochim Cosmochim Ac, 63, 2237-
1216 2245, 1999a.
1217 Waldron, S., Hall, A. J., and Fallick, A. E.: Enigmatic stable isotope dynamics of deep peat methane, Global Biogeochem
1218 Cy, 13, 93-100, 1999b.
1219 Walter, K., Chanton, J. P., Chapin, F. S., Schuur, E. A. G., and Zimov, S. A.: Methane production and bubble emissions
1220 from arctic lakes: Isotopic implications for source pathways and ages, J Geophys Res-Biogeo, 113, 2008.
1221 Walter, K. M., Zimov, S., Chanton, J. P., Verbyla, D., and Chapin, F. S.: Methane bubbling from Siberian thaw lakes as a
1222 positive feedback to climate warming, Nature, 443, 71-75, 2006.
1223 Wang, D. T., Gruen, D. S., Sherwood Lollar, B., Hinrichs, K.-U., Stewart, L. C., Holden, J. F., Hristov, A. N., Pohlman,
1224 J. W., Morrill, P. L., Könneke, M., Delwiche, K. B., Reeves, E. P., Sutcliffe, C. N., Ritter, D. J., Seewald, J. S.,
1225 McIntosh, J. C., Hemond, H. F., Kubo, M. D., Cardace, D., Hoehler, T. M., and Ono, S.: Nonequilibrium clumped
1226 isotope signals in microbial methane, Science, 348, 428-431, 2015.

Wang, D. T., Welander, P. V., and Ono, S.: Fractionation of the methane isotopologues $^{13}CH_4$, $^{12}CH_3D$, and $^{13}CH_3D$ during aerobic oxidation of methane by *Methylococcus capsulatus* (Bath), Geochim Cosmochim Ac, 192, 186-202, 2016.

Wassmann, R., Thein, U., Whiticar, M., Rennenburg, H., Seiler, W., and Junk, W.: Methane emissions from the Amazon floodplain: characterization of production and transport, Global Biogeochem Cy, 6, 3-13, 1992.

Whiticar, M., and Schaefer, H.: Constraining past global tropospheric methane budgets with carbon and hydrogen isotope ratios in ice, Philosophical Transactions of the Royal Society A: Mathematical, Physical and Engineering Sciences, 365, 1793-1828, 2007.

Whiticar, M. J., Faber, E., and Schoell, M.: Biogenic methane formation in marine and freshwater environments: CO_2 reduction *vs.* acetate fermentation—Isotope evidence, Geochim Cosmochim Ac, 50, 693-709, 1986.

Whiticar, M. J.: Carbon and hydrogen isotope systematics of bacterial formation and oxidation of methane, Chem Geol, 161, 291-314, 1999.

Woltemate, I., Whiticar, M., and Schoell, M.: Carbon and hydrogen isotopic composition of bacterial methane in a shallow freshwater lake, Limnol Oceanogr, 29, 985-992, 1984.

Worden, J. R., Bloom, A. A., Pandey, S., Jiang, Z., Worden, H. M., Walker, T. W., Houweling, S., and Röckmann, T.: Reduced biomass burning emissions reconcile conflicting estimates of the post-2006 atmospheric methane budget, Nature communications, 8, 1-11, 2017.

Yacovitch, T. I., Daube, C., and Herndon, S. C.: Methane emissions from offshore oil and gas platforms in the Gulf of Mexico, Environmental Science & Technology, 54, 3530-3538, 2020.

Young, E., Kohl, I., Sherwood Lollar, B., Etiope, G., Rumble, D., Li, S., Haghnegahdar, M., Schauble, E., McCain, K., Foustoukos, D., Sutclife, C., Warr, O., and Ballentine, C.: The relative abundances of resolved CH_2D_2 and $^{13}CH_3D$ and mechanisms controlling isotopic bond ordering in abiotic and biotic methane gases, Geochim Cosmochim Ac, 203, 2017.

Yvon-Durocher, G., Allen, A. P., Bastviken, D., Conrad, R., Gudasz, C., St-Pierre, A., Thanh-Duc, N., and Del Giorgio, P. A.: Methane fluxes show consistent temperature dependence across microbial to ecosystem scales, Nature, 507, 488-491, 2014.

Zazzeri, G., Lowry, D., Fisher, R., France, J., Lanoisellé, M., and Nisbet, E.: Plume mapping and isotopic characterisation of anthropogenic methane sources, Atmos Environ, 110, 151-162, 2015.

Zhu, J., Liu, Z., Brady, E., Otto-Bliesner, B., Zhang, J., Noone, D., Tomas, R., Nusbaumer, J., Wong, T., and Jahn, A.: Reduced ENSO variability at the LGM revealed by an isotope-enabled Earth system model, Geophys Res Lett, 44, 6984-6992, 2017.

Zimov, S., Voropaev, Y. V., Semiletov, I., Davidov, S., Prosiannikov, S., Chapin, F. S., Chapin, M., Trumbore, S., and Tyler, S.: North Siberian lakes: a methane source fueled by Pleistocene carbon, Science, 277, 800-802, 1997.